Neurochemistry International 122 (2019) 120–138

Contents lists available at ScienceDirect

Neurochemistry International

journal homepage: www.elsevier.com/locate/neuint

Tetrahydrocurcumin epigenetically mitigates mitochondrial dysfunction in brain vasculature during ischemic stroke

Nandan K. Mondal[a,b], Jyotirmaya Behera[a], Kimberly E. Kelly[a], Akash K. George[a], Pranav K. Tyagi[a], Neetu Tyagi[a,*]

[a] Department of Physiology, University of Louisville School of Medicine, Louisville, KY, 40202, USA
[b] Department of Surgery, Baylor College of Medicine, Texas Heart Institute, Houston, TX, 77030, USA

ARTICLE INFO

Keywords:
Hyperhomocysteinemia
Oxidative stress
Extracellular matrix remodeling
Tight junction protein
Blood brain barrier
Epigenetic DNA methylation

ABSTRACT

The objectives of this study are to identify the mechanism of mitochondrial dysfunction during cerebral ischemic/reperfusion (I/R) injury and the therapeutic potential of tetrahydrocurcumin (THC) to mitigate mitochondrial dysfunction in experimental stroke model. In our study, 8–10 weeks old male C57BL/6 wild-type mice were subjected to middle cerebral artery occlusion (MCAO) for 40 min, followed by reperfusion for 72 h. THC (25mg/kg-BW/day) was injected intraperitoneally once daily for 3 days after 4 h of ischemia. The experimental groups were: (i) sham, (ii) I/R and (iii) I/R + THC. We noticed that THC treatment in ischemic mice significantly improved the functional capacity and motor co-ordination along with reduced neuroscore, infarct volume, brain edema and microvascular leakage in brain parenchyma. The study revealed that level of total homocysteine (tHcy), homocysteine metabolizing enzymes, mitochondrial oxidative stress were significantly altered in I/R mice compared to sham. We also observed alteration in mitochondrial transition pore, ATP production and O_2 consumption in the ischemic brain as compared to sham. Further, elevated matrix metalloproteinases-9 (MMP-9) activity and reduced tight junction protein expressions intensified the brain vascular impairment in I/R mice compared to sham. Interestingly, we found that levels of mitophagy markers, fusion and fission proteins were significantly altered. However THC treatment in I/R mice almost normalized the above functional and molecular changes. Mechanistic study demonstrated that DNA Methyltransferase 1 (DNMT1) expression was higher and was associated with reduced mitochondrial tissue inhibitor of metalloproteinases 2 (TIMP-2) expression through hyper-methylation of CpG island of TIMP-2 promoter in I/R mice compared to sham. However, administration of epigenetic inhibitor, 5-Azacytidine (5-Aza) abrogated I/R induced hypermethylation of TIMP-2 promoter and maintaining the extracellular matrix (ECM) integrity. In conclusion, this study suggests that THC epigenetically ameliorates mitochondrial dysfunction in brain vasculature during Ischemic Stroke.

1. Introduction

According to a recent report from The American Stroke Association (AHA/ASA, 2016), nearly *800,000* people in the United States encountered stroke every year. Stroke has remained the leading cause of death globally in the last 15 years and is the second leading cause of disability, after dementia (Arnao et al., 2016). Studies reported that blood brain barrier (BBB) dysfunctions are important risk factors for ischemic stroke complications (Haley and Lawrence, 2017). Human studies have reported that elevated total homocysteine (Hcy) levels (a condition called hyperhomocysteinemia: HHcy) in acute ischemic stroke are associated with long-term mortality (Shi et al., 2015). In the body, Hcy is metabolized by three enzymes; methylene tetrahydrofolate reductase (MTHFR), S-Adenyl-L-homocysteine hydrolase (SAHH) and cystathionine γ lyase (CSE). Hypermethylation of these genes during I/R injury may lead to an increase in Hcy levels. However the role of Hcy in mitochondrial dysfunction in the context of ischemic stroke is not clear. As mitochondrion is the powerhouse of the cell, which is essential for cell survival after cerebral ischemia/reperfusion. Moreover, mitochondrion being a sensitive organelle susceptible to brain ischemia/reperfusion injury. Mitochondrial dysfunction is one of the foremost events involved in brain ischemia/reperfusion process and then induces

* Corresponding author. Department of Physiology, 500 South Preston Street, Health Sciences Centre, A-1201, University of Louisville School of Medicine, Louisville, KY, 40202, USA.
E-mail address: n0tyag01@louisville.edu (N. Tyagi).

https://doi.org/10.1016/j.neuint.2018.11.015
Received 31 July 2018; Received in revised form 7 November 2018; Accepted 20 November 2018
Available online 22 November 2018
0197-0186/

further damage to brain cells (Li and Gao, 2017). It has been shown that mitochondrial dysfunction plays a pivotal role in multiple forms of cell death, including ischemia (Pastorino et al., 1993; Zahrebelski et al., 1995), excitotoxic neurodegeneration (Beal et al., 1993), oxidant-induced stress (Dawson et al., 1993) and apoptosis (Watts et al., 2013). Previously we have shown that Hcy induces reactive oxygen species (ROS), increases the level of oxidant enzymes and reduces the levels of antioxidants enzymes in brain micro-vascular endothelial cells (Tyagi et al., 2009), even so its role in mitochondrial pathology is unclear. Interestingly, we have shown decreased CSE expression in chronic heart failure with no change in the level of cystathionine β synthase (CBS) expression (Sen et al., 2009). CBS is the key enzyme of the transsulfuration pathway for the biosynthesis of cysteine from methionine and catalyzes the condensation of Hcy and serine into cystathionine. CBS deficiency leads to abnormal accumulation of Hcy leading to HHcy (Namekata et al., 2004). Previous studies have also shown that the conversion of LC3-I to LC3-II was an indicator of autophagy activation, (in as of mitochondria it is known as mitophagy) during cardiac dysfunction (Tyagi et al., 2010; Hamacher-Brady et al., 2006). Oxidative stress has been suggested to be involved in brain edema and post-ischemic neuronal damage (Abe et al., 1988). Ischemia rapidly consumes endogenous antioxidants and produces excessive amounts of toxic free radicals (Chen et al., 2011). The accumulation of these toxic free radicals plays an essential role in blood brain barrier (BBB) disruption through matrix metalloproteinases (MMPs) activation (Gasche et al., 1999; Romanic et al., 1998).

Mitophagy denotes the degradation of mitochondria through autophagy. Autophagy is a process whereby cellular components are degraded by engulfment into an autophagosome (Chen and Chan, 2009). The existence of mitophagy has been known for some time however, whether the mitochondria are randomly or selectively targeted is unclear. Mitochondria are the site of oxidative phosphorylation and respiration, which produce reactive oxygen species (ROS) (Utsumi et al., 2003) thereby making mitochondria more prone to oxidative damage (Dawson et al., 1993; Gores et al., 1989). Hyperhomocysteinemia (HHcy) is a known contributor of oxidative damage to cellular organelles such as mitochondria (Tyagi et al., 2005), however the effect of HHcy on mitophagy, particularly, in ischemic mitochondria and its consequence on brain function has not been questioned to date. It is known that Hcy induces cerebral arteriolar stiffness, endothelium damage and finally brain dysfunction (Nappo et al., 1999).

Over the last fifty years, there has been an explosion in the literature of multiple pathways associated with neurodegeneration with respect to disease states such as stroke, traumatic brain injury, Parkinson's as well as Alzheimer's disease, among others (Watts et al., 2013). The truth is that there is no single mechanism that underlies any pathology. However, it is predicted that a majority of these pathways may be linked to energy production, either directly or indirectly. Therefore, targeting one or more of these pathways may provide protection from ischemia either by decreasing Hcy levels, severity of mitochondrial oxidative stress, mitophagy, apoptosis or by increasing mitochondrial ATP production, which may also likely benefit key pathways involved in neuroprotection/recovery. Targeting neuroprotective pathways is equally important for the treatment of ischemic stroke, so that mitochondrial dysfunction can be minimized and mitochondria specific recovery from the ischemic condition can take place.

Curcumin is the most active component of turmeric. It is believed that curcumin is a potent antioxidant and anti-inflammatory agent. Tetrahydrocurcumin (THC) is one of the major metabolites of curcumin, which exhibits many of the same physiological and pharmacological activities as curcumin and, in some systems, may exert greater antioxidant activity than curcumin (Murugan et al., 2008). Furthermore, another added benefit is that it is easily absorbed through the gastrointestinal tract (Yodkeeree et al., 2008). In addition, THC has been shown to be protective against oligomeric amyloid-β-induced toxicity in Alzheimer's disease and other neurodegenerative diseases (Murugan et al., 2008; Mishra et al., 2010; Mishra and Palanivelu, 2008). Recently it has been shown that THC also has epigenetic targeting therapeutic potential because it is a potent DNA hyomethylation agent (Liu et al., 2009a). THC treatment reduces plasma and tissue Hcy levels, thereby reducing Hcy-induced mitochondrial oxidative stress. However, the role of THC in I/R injury induced HHcy and mitophagy, mitochondrial matrix degradation and consequent vascular permeability remains unclear. Therefore, it is important to study the reparation of mitochondrial integrity and function during ischemic stroke. Additionally, the role of THC treatment in Hcy-induced mitochondria dysfunction needs to be determined to evaluate the mechanism of mitochondrial dysfunction in brain vasculature during ischemic stroke.

Epigenetic mechanisms refer to the complex and interrelated molecular processes that dynamically modulate gene expression and function within every cell in the body (Qureshi and Mehler, 2010). It is also evident that epigenetic processes are involved in the molecular and cellular mechanisms underlying stroke pathogenesis and recovery, including the deployment of stress responses that modulate cell viability and promote tissue repair and functional reorganization (Mehler, 2008). Despite decades of research, mitochondrial epigenetics remains a controversial notion. Recent findings, however, indicate that dysfunctional mitochondrial DNA (mtDNA) methylation could underlie multiple diseases (van der Wijst and Rots, 2015). Unraveling the mechanism of such a high level of regulation will be essential in understanding the role of mitochondrial epigenetics in many physiological and pathophysiological processes including ischemic stroke. Therefore, the goal of the current study was to assess the potential role of THC against the brain vascular dysfunction induced by ischemic stroke. We demonstrated that I/R enhance oxidative stress and mitochondrial dysfunction which activates MMPs and deactivates TIMPs via promoter DNA hyper-methylation. This in turn upregulates MMP-9 and subsequent alternation of tight junction proteins causing BBB alteration, and leads to brain vascular dysfunction. The administration of I/R mice with THC can mitigate these alterations and thus has a neuro-protective property.

2. Materials and methods

2.1. Antibodies

Antibodies including; CBS, CSE, MTHFR, Hcy, DNMT1 and DNMT3a were all obtained from Abcam (Cambridge, MA USA). Additional antibodies SAHH, HSP-60, Calpain-1, $p47^{phox}$, $gp91^{phox}$, TRX-2, MnSOD, TIMP-1, TIMP-2, ZO-1,Occludin, LC3, Mfn-2, Drp-1 and COXIV were purchased from Santa Cruz Biotechnology (Santa Cruz, CA, USA). GAPDH was acquired from Boster Biological Technology (Pleasanton, CA, USA).

2.2. Animal model

Wild-type male mice (strain: C57BL/6J; age: 8–10 weeks; weight: 28–33 gms.) were obtained from The Jackson Laboratory (Bar Harbor, ME) and were kept in suitable environmental conditions (12:12-h light-dark cycle, 22–24 °C) at the animal care facility of our institution. The mice were fed regular mice chow PMI®LabDiet®St Louis, MO (Cat # 5015) and water ad libitum. As the female mouse have a lower incidence of stroke compared with male which has been ascribed to protective effects of gonadal steroids, most notably estrogen. Due to the lower stroke incidence observed in female and robust preclinical evidence of neuroprotective and anti-inflammatory properties of estrogen, we have decided to focus our present study exclusively on male mice. All animal procedures were reviewed and approved by the IACUC (Institutional Animal Care and Use Committee) at the University. Moreover, methods and general guidelines for animal use were followed by the IACUC Guidelines of the NIH (National Institutes of Health).

2.3. Survival surgery: the middle cerebral artery occlusion (MCAO) and sham operation

On the day of surgery, the mice were transferred to the surgery room; MCAO was performed according to the standard operating procedures of the laboratory (Römer et al., 2015; Dirnagl, 2009). Anesthetized mice were orally intubated, mechanically ventilated and the body temperature was maintained at 37 ± 1 °C with a heating pad during surgery. The common carotid artery was exposed through a midline neck incision and dissected free of the surrounding nerves. Silicon-rubber-coated monofilament with a diameter of 0.21 ± 0.01 mm (Item # 7021910PK5Re or 7022910PK5Re; 7-0 large MCAO suture from Doccol Corporation, Sharon, MA) was introduced into the common carotid artery, advanced along the internal carotid artery to the origin of the middle cerebral artery, and left there for 40 min until reperfusion. Success of MCAO was verified applying the modified Bederson score (Bederson et al., 1986). After surgery, animals were allowed to recover in a heated cage before returning to their respective home cages. The same anesthesia and surgical procedures were performed in the sham groups of mice except the insertion of the filament. All mice were selected for sham or stroke (MCAO) surgery in a randomized manner and all analyses were performed blinded to surgical conditions.

2.4. Experimental design and THC administration

A total of 200 male mice were enrolled for the current study; among them 15 mice were excluded due to death or poor sample quality. The remaining 185 mice were grouped as follows: (i) Sham (control group; n = 60): Wild-type mice without MCAO; (ii) I/R (ischemia/reperfusion injury group; n = 60): wild-type mice with MCAO and vehicle treatment; (iii) I/R + THC (treatment group; n = 60): wild-type mice with MCAO and THC treatment. Additional mice (n = 5) were used fro I/R +5-Aza group (for mechanistic study; sub-section: 2.22). Separate studies were performed using separate groups to ensure n = 5 in each experiment. THC used in the study was purchased from Sigma-Aldrich, Inc., Saint Louis, MO, USA (Product no. SMB00370. THC was dissolved in 0.1% dimethyl sulfoxide (DMSO; Sigma, USA). THC (25 mg/kg/day) or vehicle was given for 3 days by intra-peritoneal injection after 4 h of ischemia (Tyagi et al., 2012).

2.5. Neurological deficit: assessment of neuroscore

After completion of the surgical procedure (MCAO and Sham) and subsequent recovery from anesthesia, after 72 h, neurological function was assessed according to the method of Longa et al. (1989) with slight modification. The neurological examination was evaluated by a 6-point scale as follows: 0 – no neurological deficit, 1 – failure to extend left forepaw completely showing mild focal neurological deficit, 2 – circling to the left coinciding with a moderate focal neurological deficit, 3 – falling to the left indicating a severe focal neurological deficit, 4 – not walking spontaneously and a decreased level of consciousness displayed, 5 – death due to brain ischemia. If the animal score was 0 or 5, we excluded those animals from the study.

2.6. Functional capacity: rotarod, grip test and beam balance test

To measure the motor function (balance, coordination, stamina, power production) of the experimental mice, we used a Panlab LE 8205 RotaRod System (Harvard Apparatus, Spain) according to the previously published protocol (Graber et al., 2013, 2018). In brief, experimental mice were acclimated to the device over 2 practice sessions consisting of 1 session per day with 3 trials of varied protocols per session. This was followed by a testing day where the mice ran on the device as it accelerated from 4 to 40 rpm over 5 min; the outcome measure was latency to falling. We report the best of three trials, each trial administered with a minimum 15 min rest period.

The grip strength test was used to measure the neuromuscular function in experimental mice as maximal muscle strength of combined forelimbs and hind limbs by using a grip force tester (Grip Strength Tester bio-GT3, Bioseb, Vitrolles, France) following the protocol of Larcher et al. (2014) (Larcher et al., 2014). Experimental mice were placed on their forepaws or four paws on a grid and were gently pulled backward until they released their grip (De Luca, 2008). The grip meter, attached to a force transducer, measured the peak force generated. Five tests were performed in sequence with a short latency between each test, and results were expressed in grams.

Balance beam testing was performed to evaluate sensorimotor coordination and forelimb and hindlimb functionality of experimental mice. For the balance beam test (Crabbe et al., 1985), mice were placed on a metal beam 1.3 cm diameter and 77 cm long, suspended 2 feet above the ground, and were required to traverse the beam. They were scored on a scale of 0–6 as follows: 0, crosses the beam without any slips or hesitations; 1, crosses the beam with 1 or 2 slips and/or hesitation; 2, crosses the beam partially with multiple slips and falls; 3, balances with steady posture (> 60 s) with multiple slips and 1 fall; 4, attempts to balance on the beam and falls off (> 40 s) with multiple slips and falls but walks on paws; 5, attempts to balance on the beam but falls off (> 20 s), multiple falls and fails to walk on the feet; and 6, falls off: no attempt to balance or hang on the beam (> 20 s). A score of 1 indicated strong coordination and gait, whereas a score of 6 indicated very poor performance.

Final acquisition of the data were collected at day 0, day 1, day 2 and day 3 of the experiments in three different groups of mice (sham, I/R and I/R + THC) in each case of all three functional capacity tests.

2.7. Cerebral edema: measurement of brain water content

To detect cerebral edema, the water content of brain tissues was measured by the wet and dry weight method as described previously (Fukui et al., 2003; Liu et al., 2009b; Kamat et al., 2015). Briefly, brain tissue samples from mice were immediately weighed to obtain wet weight (*WW*). The tissue was then dried in an oven at 95 °C for 72 h and weighed again to obtain the dry weight (*DW*). The formula $(WW-DW)/WW \times 100\%$ was used to calculate the water content and expressed as a percentage of wet weight (Tyagi et al., 2012).

2.8. Triphenyltetrazolium chloride (TTC) staining: assessment of brain infarct volume

Randomly selected experimental mice were euthanized and sacrificed for the detection of brain infarct volume after the completion of the study duration. Brains were quickly removed and chilled at −80 °C for 4 min to slightly harden the tissue. Five, 2-mm coronal sections were made from the olfactory bulb to the cerebellum using a mouse brain slice matrix (Harvard Apparatus, Holliston, MA, USA). The slices were stained for 30 min at 37 °C with 2% 2,3,5-triphenyltetrazolium chloride (TTC; Sigma-Aldrich, Taufkirchen, Germany) in PBS and images were captured with a digital camera to visualize the infarctions (Bederson et al., 1986; Kleinschnitz et al., 2010; Tyagi et al., 2012). The infarct size in each section was determined with a computerized image analysis program (ImageJ software, National Institutes of Health, Bethesda, MD.

2.9. Laser speckle flowmetry: measurement of cerebral blood flow (CBF) flux in the brain

Under intraperitoneal tribromoethanol (TBE @ 5 mg/kg bw) anesthesia, each animal was placed in the prone position, and the cerebral blood flow was measured using Laser Speckle Contrast Imager (Moor FLPI, Wilmington, DE) at room temperature according to the manufacturer's instructions as described previously (George et al., 2018). Briefly, a midline scalp incision was made to the anesthetized mouse

and the skull was exposed; the camera (580 9752 resolution) was positioned 15 cm from the dorsal surface of the brain. A setting for imaging was set at a display rate of 25 Hz, time constant of 1 s, and an exposure time of 4 ms. The contrast images were processed to produce a color-coded live flux image and a flux unit's trace was also recorded for 2 min in all of the animals. Data were expressed as mean CBF flux of 2 min and presented as percent change over control.

2.10. Evans Blue extravasation: evaluation of BBB integrity

We investigated the BBB integrity in experimental mice by measuring the extravasation of Evans Blue according to the established procedure (Belayev et al., 1996; Uyama et al., 1988; Kamat et al., 2015). In brief, Evans blue dye (2%, 4 mL/kg body weight) was slowly administered (at 69 h of I/R injury) via the carotid artery and was allowed to circulate for 3 h in each experimental mouse. At the end of the experiment (at 72 h of I/R injury), the mice were perfused with normal saline to wash away any remaining dye within the blood vessels. The dissected brains were weighed and extracted in 1.0 ml of 50% trichloroacetic acid solution. After homogenization and centrifugation, the extract was diluted with ethanol (1:3), and its fluorescence was determined at 620 nm (excitation) and 680 nm (emission) with a spectrophotometer (Spectra Max 3000, CA, USA).

2.11. Cranial window preparation and intravital microscopy: assessment of microvascular leakage

Blood flow in brain microvasculature was measured in anesthetized mice after 72 h of experimental condition as described in our previously published literature in detail (George et al., 2018). Prior to the creation of a cranial window for the observation of microvascular leakage, each mouse was anesthetized. A tracheotomy to maintain a patent airway and a carotid artery cannulation were performed. Each mouse was briefly placed with the head fastened in place in a stereotaxic mount (World Precision Instruments, Sarasota, FL, USA). A heating pad was used to maintain body temperature at 37 °C. Mean arterial blood pressure and heart rate were continuously monitored through a left carotid artery cannula (polyethylene tubing PE-10) connected to a transducer and a blood pressure analyzer (CyQ 103/302, Cybersense, Lexington, KY, USA). Scalp and connective tissues were removed over the parietal cranial bone. A 14-mm hole was made in the skull on the area posterior-to and lateral-to the bregma suture using a high-speed microdrill (Fine Scientific, Foster City, CA) according to the previously published procedures (Lominadze et al., 2006; Muradashvili et al., 2015). While drilling, the skull was repeatedly moistened with sterile saline to remove bone dust and to prevent overheating. The created skull flap was gently removed with a pair of forceps (Dumont &Fils #5-Fine Forceps, Switzerland) and the window was carefully cleaned with a few drops of 1 × PBS and a cotton swab. With a pair of Forceps (Dumont #5), the duramater was then carefully removed without puncturing the cortex. The surface of the exposed pial circulation was continuously superfused with 1 × PBS maintained at 37 °C by dual automatic temperature controller (Warner Instrument Corporation, Hamden, CT, USA).

Then, the mouse was fastened to the stereotaxic instrument and positioned on the stage of an Olympus BXG61WI microscope (Olympus, Tokyo, Japan) so the exposed pial circulation could be observed by incident light. Following the surgical preparation, there was a 30 min equilibration period prior to imaging. Before each experiment, autofluorescence of the observed area was recorded over a standard range of camera gains. Fluorescein isothiocyanate (FITC)-conjugated BSA (BSA-FITC-albumin, 300 mg/mL) was infused through a carotid artery cannula with a syringe pump (Harvard Apparatus, Holliston, MA) at 40 µl/min and allowed to circulate for 5 min. In vivo imaging was used to examine the exposed area of the skull. After ensuring that spontaneous leakage of BSA did not occur, venules were identified by the topology of the pial circulation and blood flow direction. Selected third order venular segments were recorded and used as the baseline. After the baseline reading was obtained, images of the venular segments were recorded. The area of interest was exposed to blue (488 nm) light for 10–15 s. The microscope images were acquired by an electron-multiplying charge-coupled device camera (Quantem 512SC, Photometrics, Tucson, AZ) and image acquisition system (Slidebook 5.0, Intelligent Imaging Innovations, Inc., Philadelphia, PA). The lamp power and camera gain settings were held constant during the experiments. Data were interpreted with the software provided with the instrument and Image-Pro Plus 6.3 software (Media Cybernetics, Bethesda, MD). Leakage of FITC-BSA was assessed by changes in the ratio of fluorescence intensity in the interstitium to the inside of the vessel. Three vessels in each animal were observed and analyzed. The results were presented as a percentage of the baseline.

2.12. Angiography: assessment of brain blood vessel architecture using barium sulfate

Barium sulfate has been widely used by radiologists to visualize the structural and motility abnormalities of blood vessel vasculature. Barium sulfate angiography was performed in mice after 72 h of experimental condition as described in our previously published procedure (Kamat et al., 2013). Barium sulfate (0.1 g/mL) was dissolved in 50 mMTris-buffer (pH 5.0) and infused slowly at a constant flow and pressure with a syringe pump through the carotid artery (Myojin et al., 2007; Givvimani et al., 2011). The brain was dissected out and placed in the X-ray chamber Kodak 4000 MM image station and angiograms were captured with high penetrative phosphorous screen by 31 KVP X-ray exposures for 3 min. Vascular density was quantified using Vessel Segmentation and Analysis (VesSeg) software tool (www.isip.uni-luebeck.de/index.php?id=150) according to the procedure of previously published literature (George et al., 2018; Pushpakumar et al., 2013).

2.13. Biochemical estimation: tHcy, CBS activity and SAM/SAH ratio

At the end of each experiment, blood was withdrawn by venipuncture of the vena cava using a 23-gauge needle and polypropylene syringe containing sodium citrate followed by our published protocol (George et al., 2018). In brief, blood was transferred to microcentrifudge tubes, then centrifuged at 1000 × *g* for 15 min to obtain supernatant plasma. Brain tissues from different experimental mice groups were also collected and homogenized in 0.1 M phosphate buffer (pH 7.4). The level of total homocysteine (tHcy) in plasma samples was measured by the mouse homocysteine kit from Crystal Chem, (Chicago, IL, USA; Catalog No.80440) according to the manufacturer's protocol. Cystathionine β-synthase (CBS) activity assay was performed in brain homogenate according to the previously published literature (Wang et al., 2004; George et al., 2018). CBS activity data were expressed as nmol/min/mg protein. S-Adenosylmethionine (SAM) and S-Adenosylhomocysteine (SAH) ELISA Combo Kit (Catalog # MBS169240, MyBioSource, San Diego, CA) was used to determine the SAM/SAH ratio in brain tissue homogenates of experimental mice according to the manufacturer's instructions. All the biochemical assays were run in triplicates.

2.14. Confocal microscopy: assessment of Hcy levels in brain tissue

Hcy levels in brain tissue during ischemia was assessed by immunohistochemistry analysis as described earlier (Tyagi et al., 2012; Qipshidze et al., 2010). In short, samples of brain tissue from all experimental groups were immediately placed onto freezing media and stored at −70 °C until they were used. Briefly, sections were post-fixed in 4% paraformaldehyde, and labeled with Hcy antibody (Abcam Antibodies, Cambridge, MA). After an overnight incubation, sections were

washed with PBS and incubated with appropriate secondary antibody conjugated with Texas Red. After washing, sections were mounted with FluoroGel mounting medium (GeneTex, Inc) and visualized with confocal microscopy (Olympus, FluoView 1000, objective 60×). DAPI was used for nuclei staining. Total fluorescence (red) intensity in 5 random fields (for each experiment) was measured with image analysis software (Image-Pro Plus, Media Cybernetics) and expressed in fluorescence intensity units (FIU). The fluorescence intensity values were averaged for each experimental group.

2.15. Preparation of brain tissue extract and protein estimation

The brain tissue from all experimental groups was homogenized in ice-cold RIPA buffer containing, PMSF (1 mM) and protease inhibitor cocktail (1 μL/ml of lysis buffer; Sigma Aldrich, St. Louis, MO, USA), then after the protein was extracted. The extract was centrifuged at 12,000×*g* for 15 min at 4 °C. The supernatant was collected, aliquoted, and stored at −80 °C until further use. Protein content in the different samples was measured with Bradford dye (Bio-Rad) in a 96-well microtiter plate against a bovine serum albumin (BSA) standard. The plate was read at 594 nm in a Spectra Max M2 plate reader (Molecular Device).

2.16. Isolation of mitochondria from brain tissue

The Mitochondria Isolation Kit (Sigma-Aldrich, Inc., Saint Louis, MO, USA; Catalog No. MITOISO01), was used to isolate mitochondria from brain tissue according to the manufacturer's instructions. All isolated mitochondria were kept on ice. The mitochondrial sub-fractions were tested for specific markers, HSP-60 for mitochondria and Calpain-1 for cytosolic fractions. The isolated mitochondrial pellet was used for Western blot and in-gel gelatin zymography.

2.17. SDS-PAGE and western blotting

Brain extracts and/or isolated mitochondrial pellets were loaded on a polyacrylamide gel and run at constant current until the dye reached the bottom. Separated proteins in the gels were transferred to polyvinylidene difluoride membranes using an electrotransfer apparatus (Bio-Rad). After blocking with 5% non-fat dry milk (1 h), the membranes were probed overnight with a primary antibody, for whole brain protein: anti-cystathionine β synthase (CBS), cystathionine γ lyase (CSE), methylene tetrahydrofolate reductase (MTHFR), S-Adenyl-L-homocysteine hydrolase (SAHH) and homocysteine (Hcy); for isolated mitochondria: anti-$p47^{phox}$, $gp91^{phox}$, thioredoxin-2 (Trx-2), mitochondrial superoxide dismutase (MnSOD), tissue inhibitor of metalloproteinases 1 & 2 (TIMP-1&2), zonula occludens-1 (ZO1), occludin, microtubule-associated protein 1A/1B-light chain 3 I & II (LC3-I&II), mitofusin-2 (Mfn-2), dynamin-related protein (Drp-1), DNA Methyltransferase 1 and 3a (DNMT1, DNMT3a)] at 4 °C. After washing, the membranes were further incubated with a secondary antibody [horse radish peroxidase-conjugated goat anti-mouse, goat anti-rabbit, or rabbit anti-goat IgG (1:2000 dilution; Santa Cruz, CA, USA)] for 60 min at room temperature. The membranes were washed and developed with ECL Western blotting detection system (GE Healthcare, Piscataway, NJ, USA). The image was recorded in the chemi-program of a gel documentation system (Bio-Rad). After that, the membranes were stripped and probed for GAPDH (for whole protein) or COXIV (for mitochondria) with an anti-GAPDH or anti-COXIV antibody (Millipore, Billerica, MA, USA) as a loading control. Each band density was normalized with a respective GAPDH or COXIV density using Image Lab densitometry software (Bio-Rad).

Table 1
List of oligonucleotide primers used for Real Time qPCR.

Gene	Accession No.	Primers
CBS	NM_144855	Forward: 5′-AGGGCTATCGCTGCATTATCGTGA-3′ Reverse: 5′-AGCTTCCACCACATAGCAGTCCTT-3′
CSE	NM_145953	Forward: 5′-CAAAGCAACACCTCGCACTC-3′ Reverse: 5′-CAGCAAGACCCGATGCAAAG-3′
MTHFR	NM_001161798.1	Forward: 5′-AGGACGGTGCGGTGAGAGTG-3′ Reverse: 5′-TGAAGGAGAAGGTGTCTGCGGGA-3′
SAHH	NM_016661.3	Forward: 5′-CACCAGATGTCCCATCGCTT-3′ Reverse: 5′-GGGAAGAGCAGAAATGGCCT-3′
$p47^{phox}$	AB002663.1	Forward: 5′-TGGATCCCAGCATCCTTCATC-3′ Reverse: 5′—CCTTGATGGCGAAGTATGGC-3′
$gp91^{phox}$	U43384.1	Forward: 5′—CCAACTGTGATAACGAGTTCA-3′ Reverse: 5′-GAGAGTTTCAGACAAGGCTTC-3′
Trx-2	NM_019913.5	Forward: 5′-AGAGTCTGTTTGACGACCTTT A-3′ Reverse: 5′-TCAGCCAATCAGCTTCTTCAGGAA-3′
MnSOD	AH005443.2	Forward: 5′-ATGACTTGTGCAAAGGTGGAAATG-3′ Reverse: 5′-GTTAAGGGGCCTCAGACTACATCC-3′
TIMP-1	NM_001294280.2	Forward: 5′-CTTGGTTCACTGGCGTACTC-3′ Reverse: 5′-ACCTGATCCGTCCACATACAG-3′
TIMP-2	NM_011594.3	Forward: 5′-TGTGGCTGCTAAATCACCA-3′ Reverse: 5′-TCATGCAGACATAATGCTGGG-3′
ZO1	NM_001163574.1	Forward: 5′- GGAGCTACGCATGCCACACT-3′ Reverse: 5′-GTCAATCAGGACTGAAACACAGTT-3′
Occludin	BC138679.1	Forward: 5′- CTCCAATGACAAAGTGAAT-3′ Reverse: 5′-CTCCCCACCTATCGTGTAGT-3′
LC3	NM_025735.3	Forward: 5′-GACCGCTGTAAGAAGGTGC-3′ Reverse: 5′-AGAAGCCGAAGGTTTCTTGGG-3′
Mfn-2	NM_001355590.1	Forward: 5′-GCAGAACTTAGTCCCAGAGC-3′ Reverse: 5′-GCCAGCTTCCTTGAAGACAC-3′
Drp-1	AB079133.1	Forward: 5′-GCAGAACTTTGTCTCAGAGC-3′ Reverse: 5′-ACCCGGAGACCTCTCATTCT-3′
DNMT-1	NM_001160045.1	Forward: 5′-AGGGAAAAGGGAAGGGCAAG-3′ Reverse: 5′—CCAGAAAACACATCCAGGGTCC-3′
DNMT3a	NM_022552.3	Forward: 5′—CCATAAAGCAGGGCAAAGACC-3′ Reverse: 5′-AGTGGACTGGGAAACCAAATACC-3′
GAPDH	NM_001289726.1	Forward: 5′-TGCACCACCAACTGCTTTGC-3′ Reverse: 5′-GGCATGGACTGTGGTCATGAG-3′
COXIV	M37829.1	Forward: 5′-TACTTCGGTGTGTCTTCGA-3′ Reverse: 5′-TGACATGGGCAACATCAG-3′

2.18. Real time qPCR: isolation of RNA, cDNA synthesis and mRNA expression

The RT-qPCR methodology was followed by our previously published protocol (George et al., 2018; Behera et al., 2018). In brief, total RNA was isolated from brain extracts and mitochondria using Invitrogen TRIzol Reagent according to the manufacturer's instructions. The quality of RNA was measured by using the NanoDrop 1000 spectrophotometer and only high quality RNA was used (260/280 > 2, 260/230 > 2) for experiments. Complimentary DNA (cDNA) was synthesized from total RNA using ImProm-II™ Reverse Transcription system kit (Promega Corporation, Madison, WI, USA). RT-qPCR was performed using the Roche LightCycler 480 Real-Time PCR according to the manufacturer's instructions. GAPDH and COXIV were used as the internal control for brain extract and mitochondria respectively. The oligonucleotide primers used for RT-qPCR are listed in Table 1.

2.19. Mitochondrial dysfunction: measurement of mitochondrial permeability transition (MPT), ATP level and O_2 consumption

To determine the extent of mitochondrial dysfunction, freshly isolated mitochondria from experimental mice were used for the measurements of mitochondrial permeability transition (MPT), ATP levels and O_2 consumption followed by previously published procedures (Moshal et al., 2008; Wang et al., 2005; Wilson-Fritch et al., 2004).

To detect MPT, isolated mitochondria were resuspended in a medium containing (in mmol/l): 180 KCl, 10 EDTA, and 10 HEPES, pH

7.4, with 0.5% BSA. To remove EDTA and BSA, the mitochondrial pellet was washed two times with wash buffer (in mmol/l: 180 KCl and 10 HEPES, pH 7.4). Mitochondrial swelling was determined by a decrease in light absorption at 540 nm with 250 μg of mitochondrial protein in swelling buffer containing (in mmol/l) 250 sucrose, 10 Tris-morpholinosulfonic acid, 0.05 EGTA, pH 7.4, 5 pyruvate, 5 malate, and 1 phosphate by the method described elsewhere (Rodrigues et al., 2002). The MPT was measured spectrophotometrically before and after the addition of $CaCl_2$ (250 μmol/l).

The levels of ATP in isolated mitochondria were measured by using the ATP Determination Kit (Invitrogen; Catalog No. A22066) according to the manufacturer's recommendations.

Mitochondrial O_2 consumption was determined by using the BD Oxygen Biosensor system (BD Bioscience, Bedford, MA) as described earlier (Wilson-Fritch et al., 2004).

2.20. Gelatinase activity: in-situ DQ-Gelatin zymography

In situ zymography gelatinolytic activity was assessed using a commercially available kit (Molecular Probes) as described previously (Tyagi et al., 2012; Gasche et al., 2001) with some modification. In brief, freshly isolated brains were frozen using 2-methylbutane with liquid nitrogen. Frozen brains were sectioned with a cryostat to a thickness of 30 μm and incubated for 3 h at 37 °C with 400 μg/mL DQ gelatin conjugate (Molecular probe), a fluorogenic substrate. After 3hr sections were washed with PBS and fixed in 4% paraformaldehyde in PBS. DQ gelatin cleaved by MMPs resulted in a green fluorescent product.

2.21. Assessment of mitochondrial MMP-9 activity

The activity of MMP-9 was assessed via our previously published procedure (Kamat et al., 2015). In brief, freshly isolated mitochondria were minced in ice-cold extraction buffer (1:3 w/v) containing 10 mMol/l cacodylic acid, 20 mMZnCl, 1.5 mM NaN_3, and 0.01% Triton X-100 (pH 5.0) and incubated overnight at 4 °C with gentle agitation. The homogenate was centrifuged for 15 min at 1500 × *g* and the supernatant was collected. 50 μg of the protein was electrophoretically resolved for each sample in 10% SDS-PAGE containing 0.1% gelatin as the MMP substrate. Gels were washed in renaturing buffer with one change in between to remove the SDS, rinsed in water, and incubated for at least 24 h in developing buffer at 37 °C in a water bath with gentle shaking. Gels were stained with 0.5% Coomassie brilliant blue for 1 h at room temperature. MMP-9 activity in the gel was detected as white bands against a dark blue background.

2.22. Mitochondrial epigenetics: assessment of DNMT activity, 5-mC, and TIMP-2 methylation analysis

To assess mitochondrial epigenetic parameters, we also included an additional ischemic mice group treated with DNA methyltransferase inhibitor, 5-Azacytidine (5-Aza). 5-Aza was dissolved in 0.9% normal saline and then injected (0.5 mg/kg body weight) to I/R mice following the same procedure as with THC treatment.

DNA Methyltransferase (DNMT) activity was ascertained according to our previously published protocol (George et al., 2018; Kalani et al., 2014), in which mitochondrial DNA extracts were isolated from the mouse brain using EpiQuik™ extraction kit (Epigentek, Farmingdale, NY, USA). DNMT activity was assessed through an EPiQuik™ DNMT activity/inhibitor assay ultra-kit (Epigentek, Farmingdale, NY, USA) according to the manufacturer's instruction. DNMT activity data was expressed as OD/h/mg of protein.

Quantification of 5-methylcytosine (5-mC) levels was used to study the global methylation profile in genomic DNA, as described in the previously published report (Kalani et al., 2014). The 5-mC levels were determined by using the 5-mC DNA ELISA kit (Zymo Research, Irvine, CA) according to the manufacturer's instructions. The result was expressed in percent (%) 5-mC in a DNA sample calculated through a standard curve generated with specially designed controls included in the kit.

We performed a bioinformatics analysis to identify CpG islands in the TIMP-2 gene by using USCS Human Genome Browser public database (http://genome.ucsc.edu) and CpG Island Explorer software (cpgie.sourceforge.net). Quantitative methylation-specific PCR (qMSP) was carried out to show the expression of methylated specific regions, particularly in CpG island regions of the TIMP-2 promoter region. The mitochondrial DNA was isolated from the experimental mice, which was followed by bisulfite conversion using Zymo EZ DNA Methylation-direct kit (Zymo Research) as per the manufacturer's instructions. A pair of primers was designed with Methprimer software/Methyl Primer Express software, to amplify bisulfite-treated methylated DNA and unmethylated bisulfite-treated DNA. The primer pairs were used to amplify sequences surroundings predicted CpG island of the TIMP-2 locus: Left M primer: AGTTATAGAAGGTAGCGGAGGAGTC, Right M primer: TTCTATCCTCTTTATCAAAAAACGC, Left U primer: TTATAGA AGGTAGTGGAGGAGTTGA, Right U primer: TCTATCCTCTTTATCAAA AAACACA. A qMSP reaction was performed to amplify the bisulfite DNA. Following PCR amplification, the PCR product was loaded onto a 1.5% agarose gel, and visualized under the gel documentation system and band intensities were normalized to unmethylated PCR products of the experimental samples.

2.23. Statistical analysis

Data analyses and graphical presentation were performed with GraphPad InStat 3 and GraphPad Prism, version 6.07 (GraphPad Software, Inc., La Jolla, CA). The data are presented as mean ± SD (standard deviation) in 5 independent experiments in all cases. The experimental groups were compared by one-way analysis of variance (ANOVA) assuming that the values were sampled from Gaussian distributions. For a set of data, if ANOVA indicated a significant difference ($p < 0.05$); Tukey-Kramer multiple comparison test was used to compare group means. Post test was only performed if $p < 0.05$. If the value of Tukey-Kramer 'q' was less than 4.046, then the p value was less than 0.05 and considered statistically significant.

3. Results

3.1. THC induced improvement of neurological score and functional capacity in ischemic mice

We checked the neuroscore to evaluate the success of the MCAO surgery and the effect of THC on its recovery. The neuroscores were significantly decreased in THC treated mice as compared to the I/R group (Fig. 1a). Latency to fall off the RotaRod, as an indicator of motor function, were similar in all three groups prior to sham and MCAO surgery (day 0). After the surgical procedure, on day 1, the RotaRod fall latencies were lowered in all three groups, but the I/R group was significantly decreased compared to others. Temporal data indicated that the deficit appeared to recover over time (day 2 and 3) in sham and I/R + THC group compared day 1; while the changes (day 1 to day 2 to day 3) were not prominent in I/R group (Fig. 1b). The grip strength test was used to measure neuromuscular function and appeared to be comparable in all three groups at baseline (day 0). Temporal comparative data of grip strength test revealed a similar trend as with RotaRod data indicating THC mediated improvement of neuromuscular function in ischemic mice (Fig. 1c). The beam balance score indicated strong coordination and gait at baseline in all three groups, whereas very poor performance was found in the I/R group compared to sham and THC treated groups (Fig. 1d). Thus, THC treatment effectively improved the sensorimotor coordination and forelimb and hindlimb functionality of I/R mice.

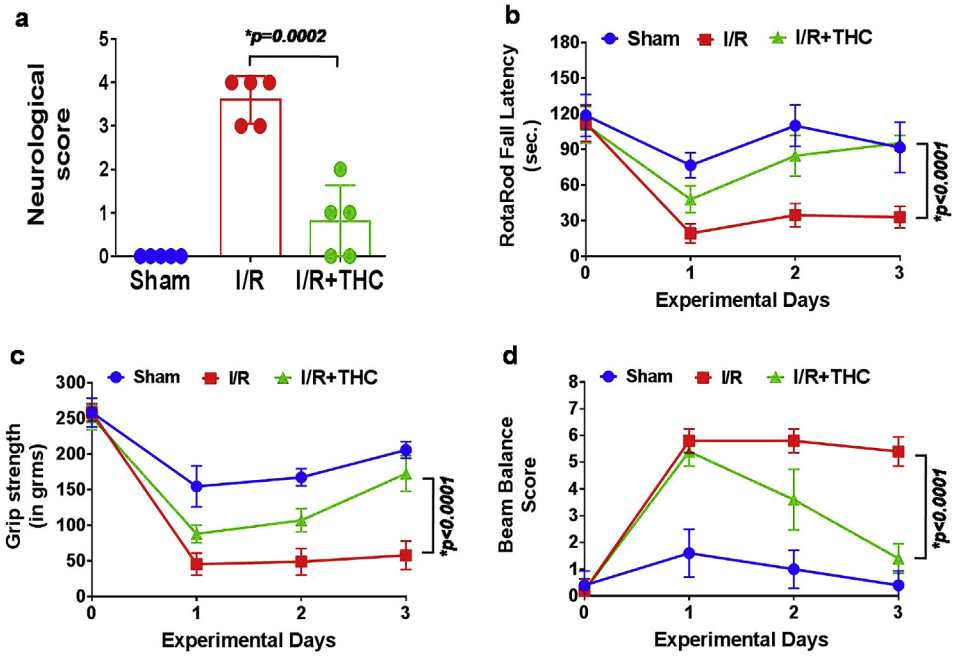

Fig. 1. Neuroprotective effects of THC in ischemic stroke. Histogram showing neuroscore of sham, I/R and I/R + THC-treated mice measured 72 h after MCAO or sham surgery (a). Comparative line graphs for the temporal data points of RotaRod fall latency (b), grip strength (c) and beam balance score (d) in sham, I/R and I/R + THC mice. Experimental data are presented as mean ± SD (standard deviation) and *, $p < 0.05$ is considered significant (n = 5 mice per group).

3.2. Effect of THC on brain edema, cerebral infarction and blood flow in the ischemic brain

To indicate I/R induced brain injury, cerebral edema was confirmed by measuring water contents in cortical areas. We found a significant increase in water content of the cortex of ischemic brains as compared to the sham operated group (https://www.ncbi.nlm.nih.gov/pmc/articles/PMC4567529/figure/F1/,Fig. 2a). Furthermore, the brain infarct volume was significantly increased (pale-colored region) in the ischemic group as compared to the sham-operated control group (Fig. 2b and c). A remarkably decreased pale-colored region was observed in the THC-treated mice brain as compared with the ischemic brain indicating recovery of I/R induced brain injury. Ischemic stroke induced vasoconstriction reduces cerebral blood flow and can cause vascular damage. In the current study, we measured cerebral blood flow in all three groups of mice. The result showed that cerebral blood flow in the I/R brain was significantly reduced compared to sham, and THC treatment ameliorated this change (Fig. 2d and e).

3.3. Effect of THC on cerebrovascular permeability in the ischemic brain

To elicit the effect of THC treatment on cerebrovascular permeability, we quantified the extravasation of Evans blue dye in the experimental brain as an indicator of blood brain barrier (BBB) breakdown. The levels of Evans blue dye were significantly increased in I/R group as compared to the sham-operated group; while the extravasation of Evans blue dye was significantly decreased in THC treated mice as compared to ischemic only mice (https://www.ncbi.nlm.nih.gov/pmc/articles/PMC3609416/figure/F2/,Fig. 3a and b).

To determine whether THC treatment alleviated the BBB permeability in the I/R mouse brain, we measured the interstitial diffusion of BSA (FITC-labeled) in experimental brains by intra-vital microscopy. We detected that the BBB permeability was significantly higher in the I/R group as compared to the sham operated brain. THC treatment reduced BBB permeability in the I/R + THC brain and reduced FITC-BSA leakage was observed in these brains (https://www.ncbi.nlm.nih.gov/pmc/articles/PMC3966971/figure/F8/,Fig. 3c and d). These results suggest that cerebral ischemia was associated with increased permeability in the brain interstitial parenchyma and that this damage was partially prevented by THC treatment.

Additionally, barium sulfate angiography of experimental mouse brains showed that there was a significant increase in vascular permeability in the I/R group when compared with the sham group as evident from the reduced % of vascular area in I/R group. However, THC treatment partially restored vascular patency in the I/R + THC group (Fig. 3e and f). All three experimental data are in general agreement that THC could improve post-ischemic brain injury by decreasing cerebrovascular permeability.

3.4. Ischemic reperfusion injury interferes with Hcy metabolism leading to HHcy and THC treatment reversed the effect

In order to evaluate the role of THC treatment on the HHcy condition induced by ischemia, we analyzed the Hcy levels in brain tissue and in plasma of experimental mice groups. Further, to know the effect of THC on the metabolic regulation of the ischemia induced Hcy pathway; we quantified CBS activity, SAM/SAH ratio and the crucial enzymes: cystathionine β-synthase (CBS), cystathionine γ-lyase (CSE), Methylene tetrahydrofolate reductase (MTHFR), S-Adenyl-L-homocysteine hydrolase (SAHH) and homocysteine (Hcy) involved in methionine metabolism. Tissue and total plasma Hcy levels were robustly increased in I/R groups as compared to sham. The THC treatment demonstrated a decrease in Hcy levels in the ischemic brain and circulation (Fig. 4a–c). Biochemical estimation of CBS enzyme activity data indicated that compared to sham, I/R mice had significantly lowered CBS activity; while THC treatment reversed CBS activity to sham level in the I/R + THC group (Fig. 4d). The SAM/SAH ratio was found to be significantly higher in I/R mice compared to sham, while THC treatment in I/R mice significantly reduced the SAM/SAH ratio compared to sham (Fig. 4e). Western blot analysis also revealed that the protein levels of CBS, CSE, and MTHFR were significantly decreased while the level of SAHH was significantly increased in I/R mice compared to sham. THC treatment ameliorated these changes to control levels (Fig. 4f and g). Additionally, the q-PCR analysis of CBS, CSE, MTHFR and SAHH mRNA expression confirmed our protein data (Fig. 4h–k). Collectively, these results suggest that I/R mediated altered expression of enzymes involved in the Hcy metabolism and THC treatment restored the altered levels of Hcy, CBS, CSE, MTHFR and SAHH.

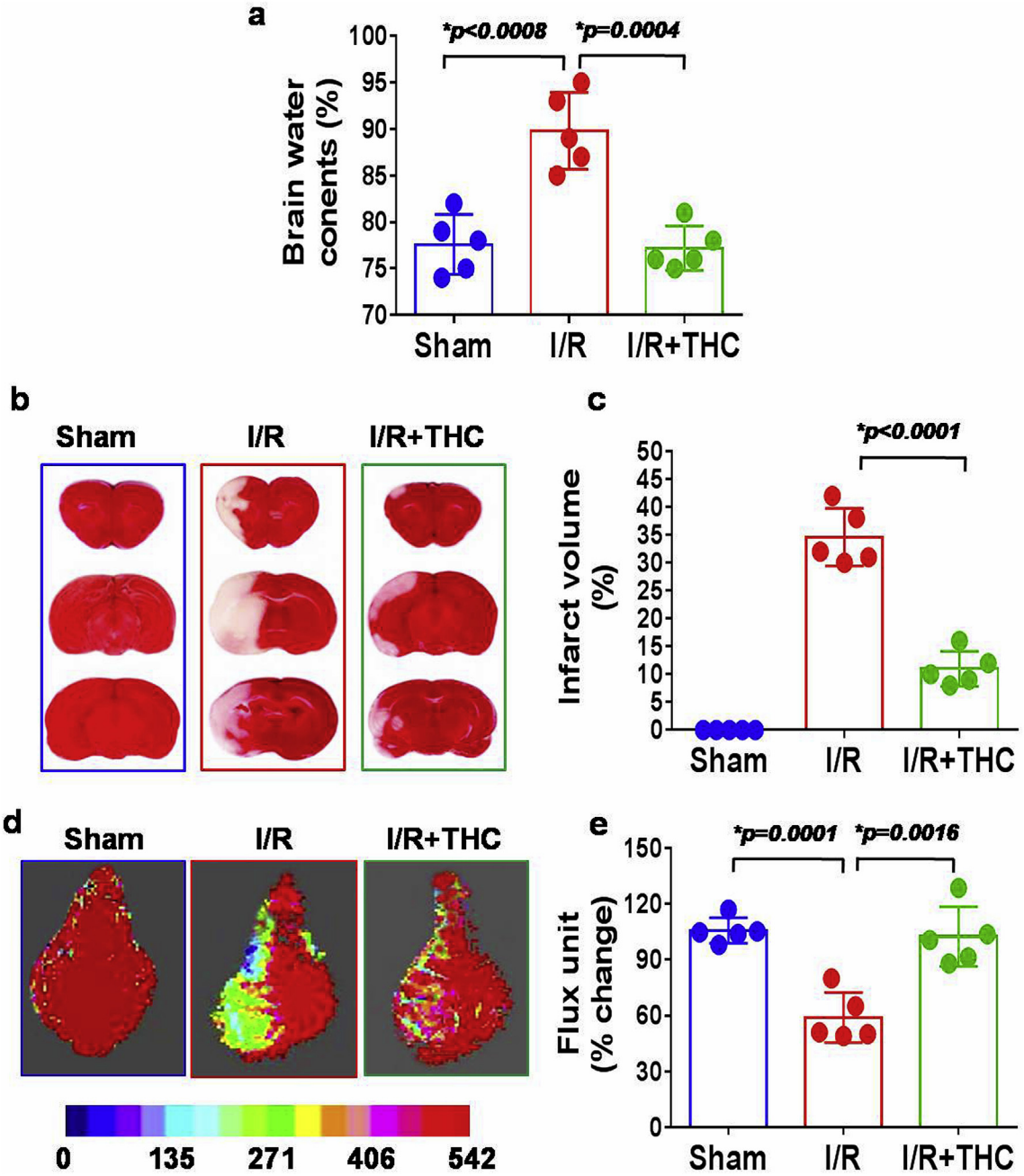

Fig. 2. Effect of THC on brain edema, cerebral infarction and blood flow in the ischemic brain. Histogram showing comparison of brain edema in sham, I/R and I/R + THC groups (a). Representative coronal sections stained with 2% TTC after 40 min of MCAO and 72 h of reperfusion showing infarction. Dark colored region indicates no-ischemic portion of brain and pale-colored region indicates ischemic portion of the brain (b). Histogram showing differences in infarct volume between sham, I/R and I/R + THC groups (c). Representative images showing microvascular density in the brain using laser Doppler flow in different groups of mice (d). Histogram showing flux units of microvascular density captured in the 6 different areas of the cranial window prepared in different groups of mice (e). Experimental data are presented as mean ± SD (standard deviation) and *, $p < 0.05$ is considered significant (n = 5 mice per group).

3.5. Effect of THC on mitochondrial oxidative stress in the ischemic brain

In order to know the effect of THC on mitochondrial oxidative stress in the ischemic brain; protein and mRNA levels of crucial mitochondria specific oxidant ($p47^{phox}$, $gp91^{phox}$) and anti-oxidant (Trx-2, MnSOD) enzymes were quantified in isolated mitochondria from experimental mice brains (Fig. 5). To determine the mitochondrial viability, function and respiration, the mitochondrial fractions from experimental mouse brains were isolated and checked for their purity by using Western blot analysis (Fig. 5a). Our data indicated that protein and mRNA levels of $p47^{phox}$ and $gp91^{phox}$were significantly elevated in I/R mice when compared to sham mice (Fig. 5b–g). On the other hand, the levels of Trx-2 and MnSOD were significantly reduced in the I/R group compared to the sham group. These data indicated that there was an imbalance between oxidant and anti-oxidant status in I/R mice, indicating mitochondrial oxidative stress. Data also indicated that treatment with THC alleviated the severity of oxidative stress in the I/R + THC group (Fig. 5).

3.6. Effect of THC on mitochondrial dysfunction in the ischemic brain

Ischemic reperfusion induced the increase in mitochondrial

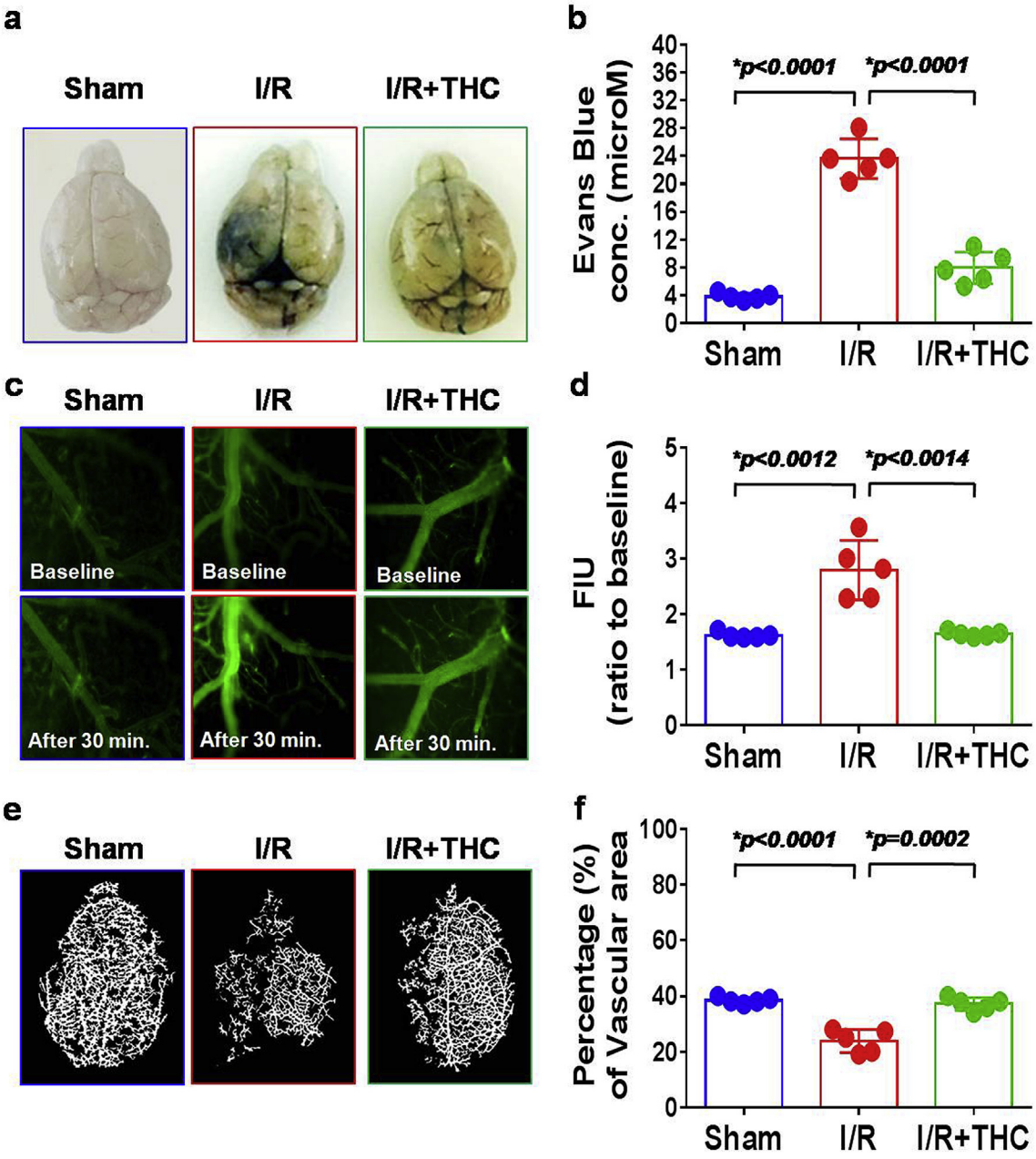

Fig. 3. Effect of THC on cerebrovascular permeability in the ischemic brain. Whole brain images showing the extent of extravasation of Evans blue dye in experimental mice (a). Histogram showing quantitative analysis of the extravasation of Evans blue dye after 45min of MACO and 72hrs of reperfusion (b). Representative images showing fluorescent protein (FITC-BSA) leakage from pial vessels into the brain parenchyma – indicating alteration in microvascular permeability in different groups of mice (c). Histogram showing quantitative estimation of fluorescent intensity unit (FIU) in different groups of mice after FITC-BSA injection (d). Representative images of cerebral angiogram with barium sulfate contrast in different groups of mice (e). Histogram showing the pattern of vascular density in the form of percentage of vascular area in different groups of mice (f). Experimental data are presented as mean ± SD (standard deviation) and *, $p < 0.05$ is considered significant (n = 5 mice per group).

permeability transition (MPT) pore in brain mitochondria. Interestingly, the I/R-induced increase in MPT was attenuated by THC treatment after 45 min of middle cerebral artery occlusion and 72 h of reperfusion (Fig. 6a).

To distinguish if there are any changes in ATP levels, which is the main currency for cell function, we assayed for the levels of ATP in the brain mitochondria of experimental mice. We noticed a considerable decrease in ATP levels in the ischemic mice compared to sham, while THC treatment ameliorated these changes (https://www.ncbi.nlm.nih.gov/pmc/articles/PMC4372482/figure/F4/,Fig. 6b). These findings gave us indications that ischemia might compromise either mitochondrial function or biogenesis and is responsible for the lower ATP production in I/R mice, as mitochondrial oxidation is the biggest contributor to cellular ATP production.

Alternation in MPT can alter the rate of oxygen consumption. We measured oxygen consumption using BD Biosciences Oxygen Biosensor System. The entire plate was pre-blanked and then mitochondria were seeded into the plate. As shown in https://www.ncbi.nlm.nih.gov/pmc/articles/PMC2921889/figure/F3/, Fig. 6c, I/R decreased the oxygen consumption compared to sham. Importantly, the I/R-mediated decrease in oxygen consumption was mitigated by THC treatment (https://www.ncbi.nlm.nih.gov/pmc/articles/PMC2921889/figure/F3/,Fig. 6c).

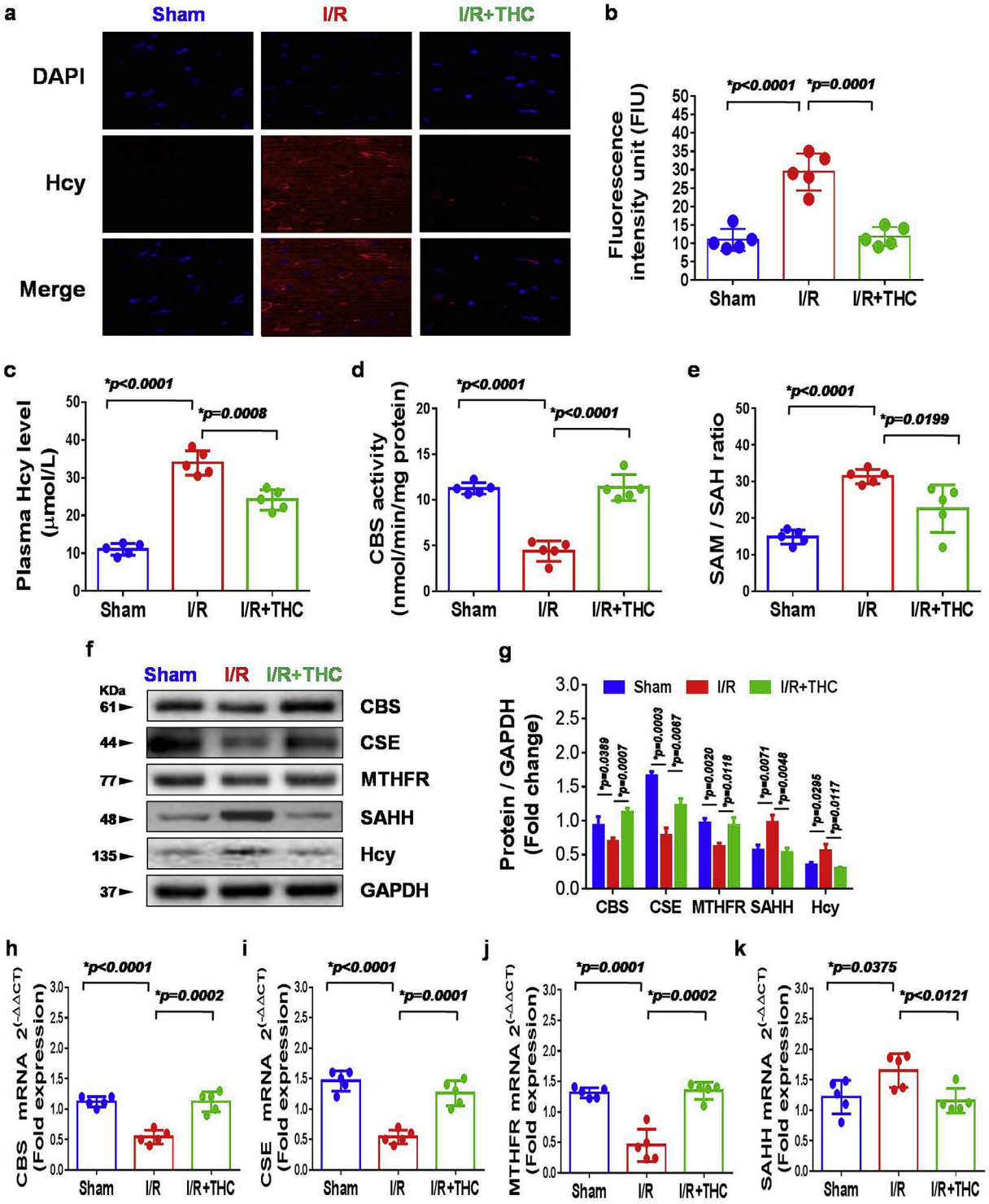

Fig. 4. Ischemic reperfusion injury interferes with Hcy metabolism leading to HHcy and THC treatment reversed the effect. Typical immunohistochemistry on brain sections for Hcy (red) counterstained with DAPI (blue) (a). Histogram showing elevated fluorescence intensity for Hcy in I/R group compared to sham and I/R + THC groups (b). Histograms showing biochemical analysis of plasma Hcy (c), CBS activity (d) and SAM/SAH ratio (e) in experimental mice. Representative western blot analysis for the vital enzymes (CBS, CSE, MTHFR, SAHH and Hcy) involved in homocysteine metabolism in different groups of mice (f). Bar graphs showing quantitative estimation of key proteins after normalization with GAPDH (g). The q-PCR analysis showing the data for real-time transcript levels of CBS (h), CSE (i), MTHFR (j) and SAHH (k) mRNAs in different groups of mice. Experimental data are presented as mean ± SD (standard deviation) and *, $p < 0.05$ is considered significant (n = 5 mice per group).

3.7. Effect of THC on mitochondrial extracellular matrix (ECM) remodeling and tight junction proteins (TJP) alteration in the ischemic brain

Matrix metalloproteinase-9 (MMP-9), also known as gelatinase, is a matrixin, a class of enzymes that belong to the zinc-metalloproteinases family involved in the degradation of the extracellular matrix (Lu et al., 2011). MMP-9 is a known marker for cerebral injury. To assess total MMPs activity, in situ DQ-gelatin zymography was performed in fresh

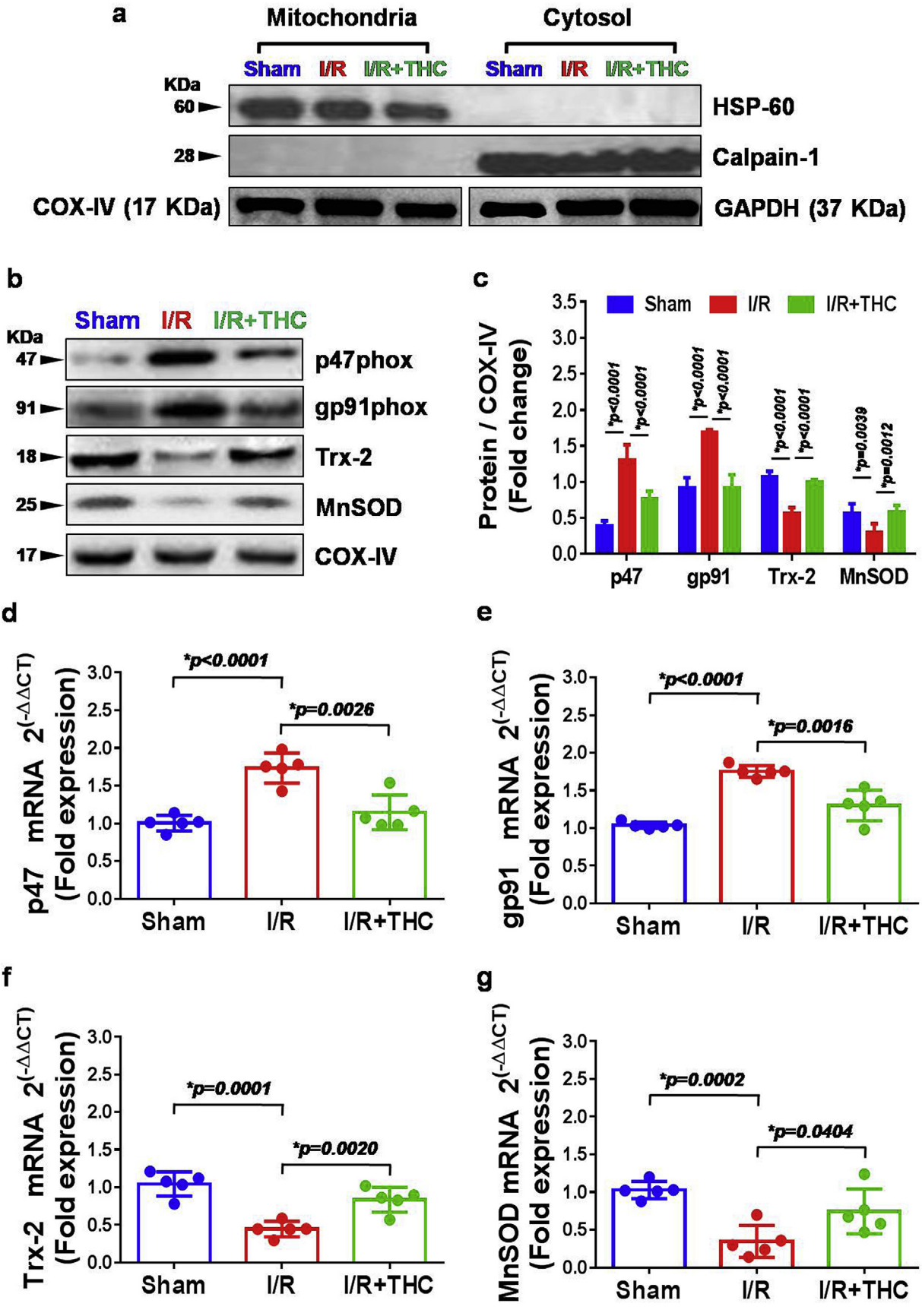

(caption on next page)

Fig. 5. Effect of THC on mitochondrial oxidative stress in the ischemic Brain. Mitochondrial and cytosolic fractions were characterized by heat shock protein (HSP-60) in mitochondria and Calpain-1 in the cytosol by western blot analysis. COXIV was used as loading control for mitochondrial fractions and GAPDH for cytosolic fractions (a). Representative western blot analysis from isolated brain mitochondria showing the levels of mitochondria specific oxidant ($p47^{phox}$, $gp91^{phox}$) and anti-oxidant (Trx-2, MnSOD) proteins in different groups of mice (b). Bar graphs showing the quantitative estimation of mitochondrial oxidative stress specific proteins after normalization with COX-IV (c). The q-PCR analysis showing the data for real-time transcript levels of $p47^{phox}$, $gp91^{phox}$Trx-2, and MnSOD mRNAs in different groups of mice (d–g). Experimental data are presented as mean ± SD (standard deviation) and *, $p < 0.05$ is considered significant (n = 5 mice per group).

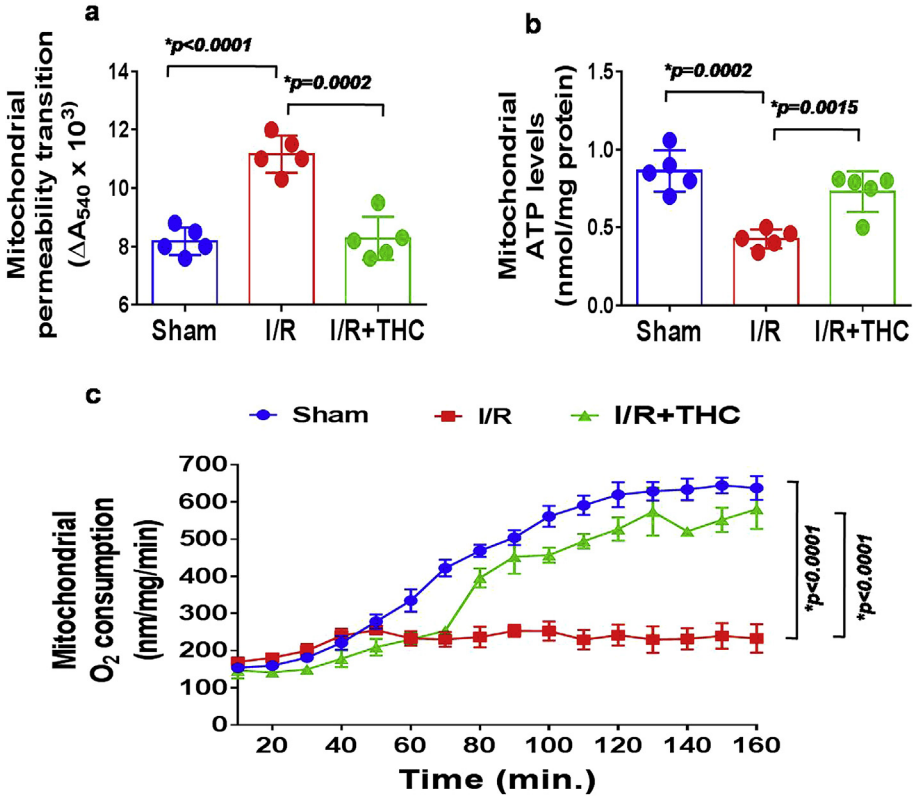

Fig. 6. Effect of THC on mitochondrial dysfunction in the ischemic brain. Measurements of mitochondrial permeability transition (MPT) pore: the mitochondria from sham, I/R and I/R + THC groups were isolated and suspended in swelling buffer (pH7.4) $CaCl_2$ was added to initiate the swelling, and the absorbance was recorded at 540 nm (A540). The δA540 (A540max − A540min) was calculated and plotted (a). Histogram showing comparison of mitochondrial ATP levels in the brain among sham, I/R and I/R + THC groups (b). Mitochondrial oxygen (O_2) consumption was measured by gradual increase in fluorescence at 630 nm when excited at 485 nm as mitochondrial capacity to utilize the oxygen using oxygen-sensitive fluorescent dye, tris(4,7-diphenyl-1,10 phenanthroline) ruthenium (II) chloride, embedded in a gas-permeable silicone polymer matrix affixed to each well bottom of a standard Falcon microplate (BD Oxygen Biosensor system). The change in fluorescence with time was measured and presented as line graphs for the sham, I/R and I/R + THC groups (c). Experimental data are presented as mean ± SD (standard deviation) and *, $p < 0.05$ is considered significant (n = 5 mice per group).

brain slices from all groups. There was a marked increase in gelatinolytic activity in the ischemic group as compared to sham operator groups (Fig. 7a). It is clear that, gelatinolytic activity was reduced in the THC treated groups (Fig. 7a). Interestingly, matrix extracted from isolated mitochondria of the ischemic brain also showed an increase in MMP-9 activity in gelatin-gel zympgraphy while THC treatment ameliorated this MMP-9 activity (Fig. 7b). These results suggested that THC treatment significantly inhibited the induction of MMP-9 activity (Fig. 7a and b). We did not notice any significant change ($p > 0.05$) in TIMP-1 protein and mRNA levels between the three experimental mice groups (Fig. 7c and d). However, we noticed a significant decrease in TIMP-2 proteins in the I/R group compared to sham and THC treatment ameliorated these changes (Fig. 7c). Gene expression via q-RT-PCR analysis also revealed a reduced TIMP-2 expression in the ischemic brain (Fig. 7e). To determine whether tight junction proteins (Zona occluden-1 [ZO1] and Occludin) are MMP targets, we determined TJP protein expression by Western blot analysis in brain lysates. The results showed down regulation of ZO1 and Occludin in the ischemic brain, which was mitigated by THC treatment (Fig. 7c). Additionally, the q-PCR analysis of ZO1 and Occludin mRNA expression confirmed our protein data (Fig. 7f and g). Collectively, these results suggest THC treatment normalized the mitochondrial ECM and subsequent tight junction proteins alteration in brain cells.

3.8. Effect of THC on mitochondrial dynamics in ischemic brain

To support the claim of mitophagy occurrence in ischemic brains, the levels of mitophagy markers (conversion of LC3-I to LC3-II in mitochondria) Mfn-1 (mitofusin-1, fusion protein) and Drp-1 (dynamin-related protein-1, fission protein) were measured by Western Blot (Fig. 8a and b). LC3-II increased in ischemic mitochondria whereas Mfn-1 and Drp-1 protein expression were decreased in ischemic mitochondria. THC treatment inhibited the conversion of LC3-I to LC-3-II and enhanced the expression of Mfn-1 and Drp-1 (Fig. 8a and b). Additionally, the gene expression (q-RT-PCR) analysis of LC3, Mfn-1 and Drp-1 confirmed our protein data (Fig. 8c–e). This finding suggested that ischemia induced changes in mitochondrial dynamics were restored by the THC treatment.

3.9. Ischemia-induced epigenetic remodeling through TIMP-2 hypermethylation: role of THC and DNMT inhibitor 5-aza

To understand the effect of THC treatment on epigenetic changes in brain mitochondria, we measured the protein and mRNA levels of DNA methyltransferase 1 (DNMT1) and DNA methyltransferase 3 alpha (DNMT3a) by western blotting and qPCR in the brain mitochondrial extracts of experimental mice groups. The results revealed that, DNMT1 and DNMT3a protein and mRNA levels were significantly increased under ischemic conditions when compared to the sham group. However, THC treatment in ischemic mice was able to reverse the I/R mediated increase in DNMTs expression (Fig. 9a–d). Additionally, biochemical estimation of DNMT activity in experimental mice confirmed our protein and mRNA data (Fig. 9e). Further, we determined global DNA methylation from the isolated mitochondrial extracts derived DNA, using 5-mC ELISA. The data suggest that the % 5-MC level was higher in I/R mice compared to with sham group. (Fig. 9f). The

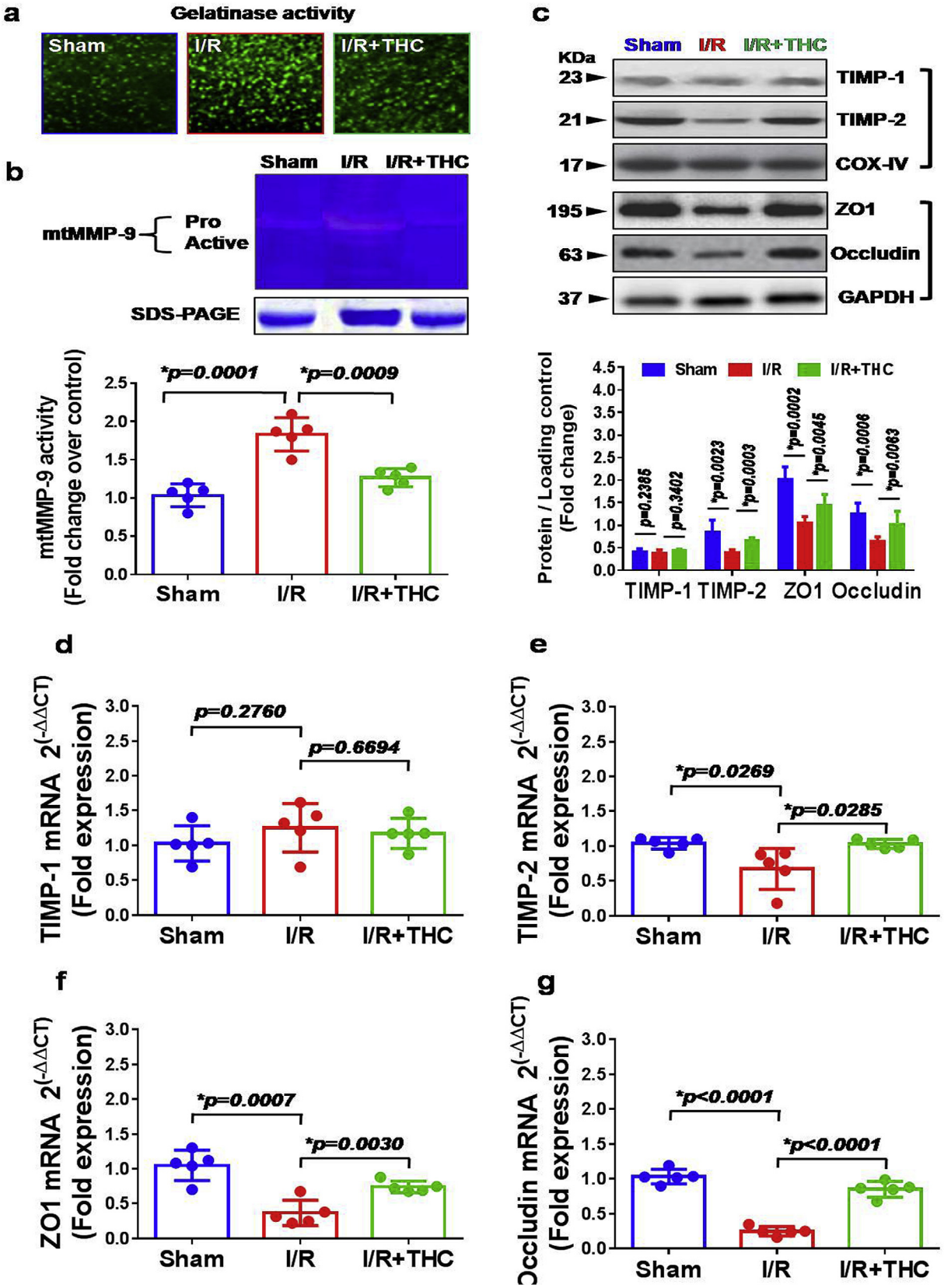

Fig. 7. Role of THC on extracellular matrix remodeling and tight junction proteins in the ischemic brain. Representative photomicrographs of gelatinase activity in brain sections of sham, I/R and I/R + THC groups (a). Gel panel image of in-gel gelatin zymography for MMP-9 activity and corresponding SDS-PAGE used as loading control in brain mitochondrial fractions and corresponding densitometric analysis plotted as a histogram as fold change to control (b). Representative western blot analysis from isolated brain mitochondria (TIMP-1&2) and brain lysate (ZO1, Occludin) showing the levels of TIMP-1, TIMP-2, ZO1 and Occludin proteins in different groups of mice. The COX-IV (for mitochondria) and GAPDH (for brain lysate) normalized corresponding histogram for densitometric analyses are shown (c). The q-PCR analysis showing the data for real-time transcript levels of TIMP-1, TIMP-2, ZO1 and Occludin mRNAs in different groups of mice (d–g). Experimental data are presented as mean ± SD (standard deviation) and *, $p < 0.05$ is considered significant (n = 5 mice per group).

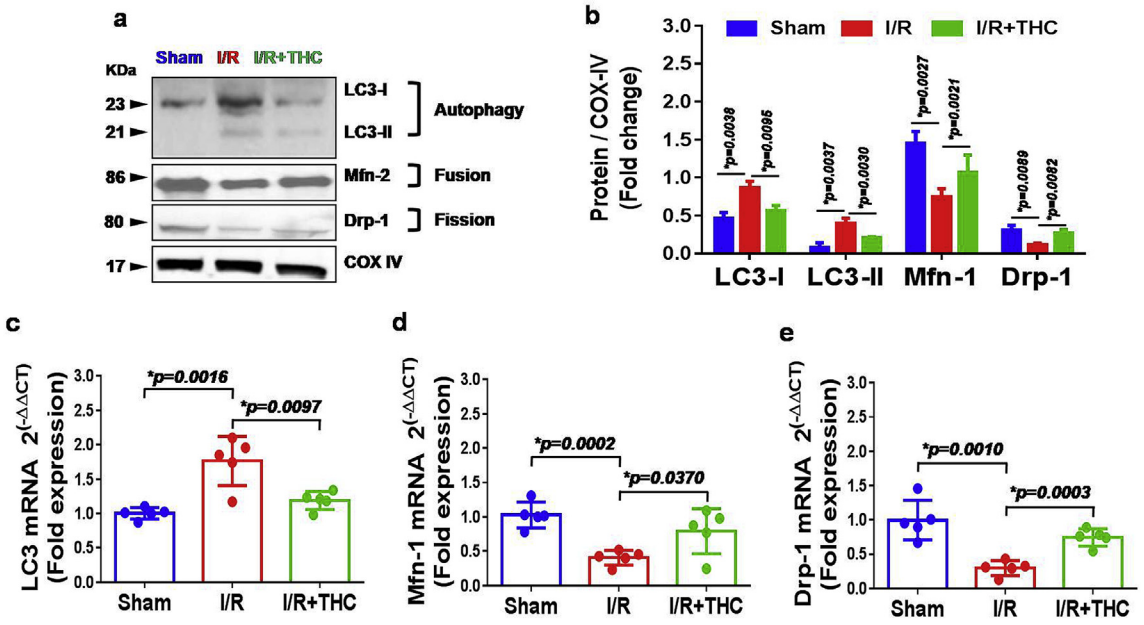

Fig. 8. Effect of THC on mitochondrial dynamics in the ischemic brain. Immunobloting for cleaved LC3 (LC3-II) using brain mitochondrial fractions from sham, I/R and I/R + THC groups (a). Bar graphs showing quantitative estimation of key proteins after normalization with COXIV loading control (b). The q-PCR analysis showing the data for real-time transcript levels of LC3 (c), Mfn-1 (d) and Drp-1(e) mRNAs in different groups of mice. Experimental data are presented as mean ± SD (standard deviation) and *, $p < 0.05$ is considered significant ($n = 5$ mice per group).

CpG island prediction in theTIMP-2 gene promoter was performed by USCS Human Genome Browser public database/Methprimer analysis (Fig. 9g). As the increased DNMT activity may regulate methylation patterns in CpG islands of TIMP-2 promoters under ischemic condition, I/R mice were treated with either THC or 5-Aza (DNMT inhibitor) and the DNA methylation pattern in the TIMP-2 promoter was measured by quantitative methylation specific PCR (qMSP-PCR). The result revealed a significant increase in the DNA methylation of the CpG regions of the TIMP-2 promoter of I/R mice as compared to sham; and THC or 5-Aza treatment reversed this effect in I/R + THC or I/R+5-Aza mice (Fig. 9h). To dissect further the involvement of an epigenetic mechanism, we tested the levels of DNMT proteins, mRNAs and activity with 5′-Aza (DNMT inhibitor) treatment in separate experimental mice. Our data showed that 5-Aza or THC treatment significantly decreased DNMT activity and expression in ischemic mice compared to sham (Fig. 9).

4. Discussion

Progress in the field of mitochondrial dysfunction in the past few years has shown that mitochondrial activities go beyond bioenergetics (Hagberg et al., 2014). The new aspects of mitochondrial dynamics and dysfunction have important implications for the ischemic brain. On one hand, the present study provides the basic understanding of a new mechanism of mitochondrial dysfunction during I/R injury through hyperhomocysteinemia induced impairment in mitochondrial remodeling, while on the other-hand also suggests that high levels of Hcy may be a marker or may influence brain function during cerebral I/R. The therapeutic success by THC in ischemic mice may determine whether they are candidates for clinical trials in I/R injury or not. To the best of our knowledge, the present study demonstrates for the first time that THC treatment is not only a neuroprotectant but also may be considered as an inducer of recovery after stroke.

In this study, we have shown that THC induced improvement of neurological scores and functional capacity in ischemic mice. Assessing functional outcomes in preclinical studies of stroke has become increasingly recognized (Schaar et al., 2010). The variety of deficits that accompany stroke requires a diversity of behavioral tests, from global to modality specific. Overall, tests should be sensitive to the location of injury, extent of damage, and beneficial treatment (Schallert et al., 2000). We found that balance, coordination, stamina, power production, neuromuscular function, sensorimotor coordination and forelimb and hindlimb functionality were significantly improved in ischemic mice group treated with THC, indicating a potential therapeutic role of THC in ameliorating ischemia (Fig. 1). As pre-stroke neuroscores for all the mice from 3 groups were same (score 0) indicating no neurological deficit. The neuroscore data immediately after stroke were comparable in I/R and I/R + THC group (Score: 3/4). The neuroscore in I/R mice with THC treatment improved compared to I/R only at day 3. Thus, we only presented the data of neuroscore at day 3 in all 3 groups. Our data indicated that THC treatment decreased brain edema, infarct volume, cerebral blood flow and improved blood brain barrier (BBB) damage after ischemic stroke. Other studies have shown that disruption of the BBB occurs under various pathological conditions such as I/R injury, which may cause an increase in vascular permeability with subsequent development of brain edema (Utepbergenov et al., 1998). Protection of the BBB has become an important experimental therapeutic target during ischemic stroke (Veltkamp et al., 2005). In the present study, our results indicate that THC inhibited the neurotoxicity of ischemic reperfusion by decreasing water content of the brain and prevented the absorbance of Evans blue dye after I/R injury, suggesting that THC protects BBB integrity by reducing endothelial cell damage (https://www.ncbi.nlm.nih.gov/pmc/articles/PMC3609416/figure/F2/,Figs. 2 and 3).

Numerous studies have demonstrated that total homocysteine (Hcy) is a strong, graded, and independent risk factor for coronary heart disease and stroke (Casas et al., 2005; Wald et al., 2002; Bostom et al., 1999; Iso et al., 2004). Studies have also demonstrated that elevated Hcy levels are associated with higher mortality rates from stroke and coronary heart disease (Sacco et al., 2004; Cui et al., 2007). In our study, we noticed that total plasma and tissue Hcy levels were robustly increased in ischemic groups as compared to sham. The THC treatment demonstrated a decrease in Hcy levels in the ischemic brain (Fig. 4). Moreover, we also noticed that the ischemic stroke induced an alteration in the expression of enzymes involved in Hcy-metabolism such as CBS, CSE, MTHFR, and SAHH (Fig. 4). In particular, Hcy levels are

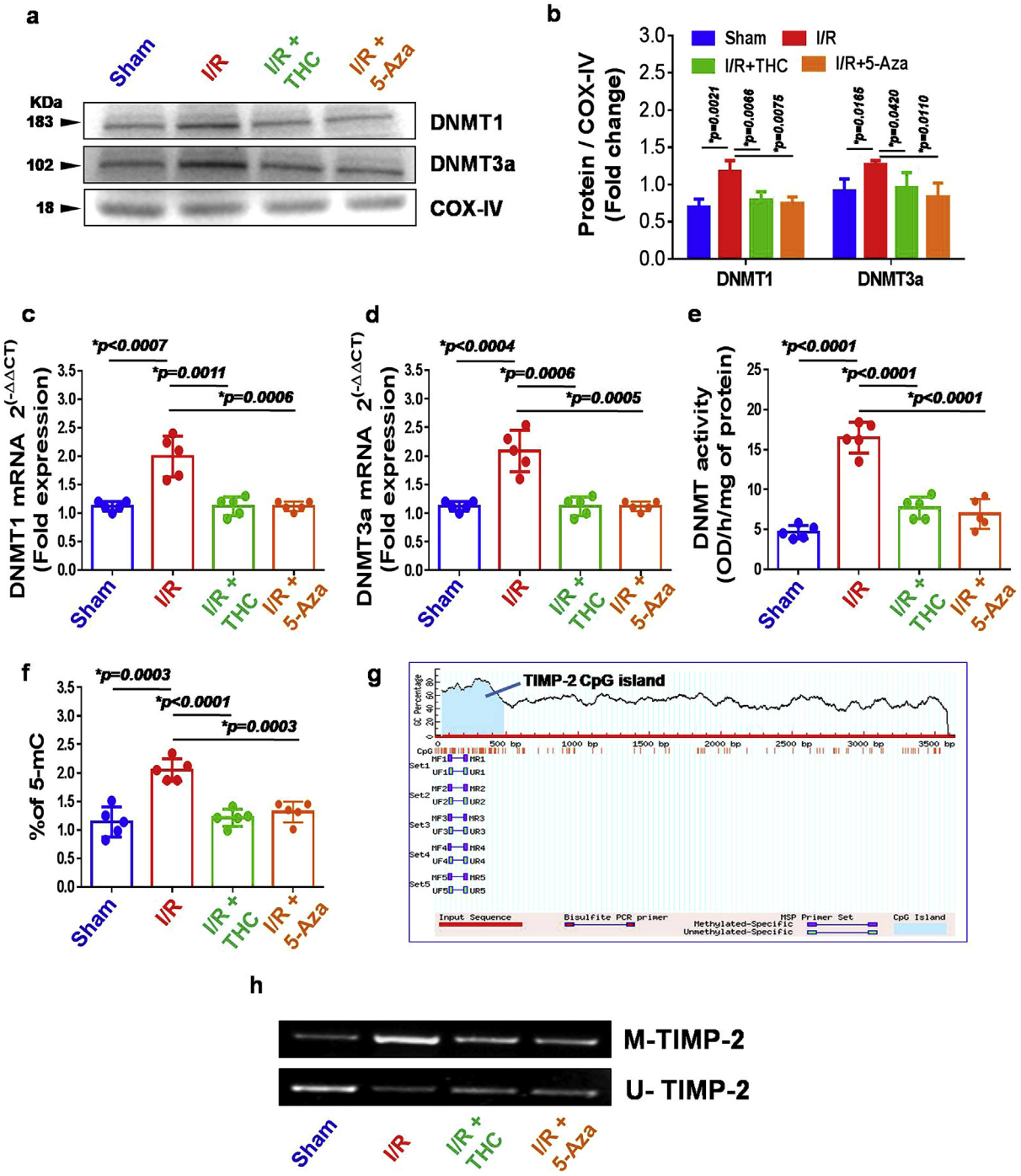

Fig. 9. Effect of THC and 5-Aza on ischemia-induced epigenetic remodeling through TIMP-2 hypermethylation. Representative western blot analysis showing the levels of DNMT1 and DNMT3a in mitochondria extracted from brain tissue of different mice groups (a). Histogram showing the quantitative estimation of DNMT1 and DNMT3a proteins after normalization with COX-IV (b). The q-PCR analysis showing the data for real-time transcript levels of DNMT1 and DNMT3a mRNAs in the different groups of mice (c,d). Histogram representing the DNMT activity in brain samples of different mice groups (e). Histogram representing global DNA methylation status by % 5-mC detected in different mouse brain mitochondrial DNA samples (f). Schematic diagram of the CpG island prediction in the TIMP-2 gene promoter was performed by USCS Human Genome Browser public database/Methprimer analysis (g). Bisulfite-modified DNA derived from brain mitochondria were amplified with TIMP-2 primers specific for unmethylated and methylated DNA in sham, I/R and I/R mice treated with either THC alone and DNMT inhibitor 5-Aza alone. M-TIMP-2, primers specific for methylated TIMP-2 DNA; U-TIMP-2, primers specific for unmethylated TIMP-2 DNA (h). Experimental data are presented as mean ± SD (standard deviation) and *, $p < 0.05$ is considered significant (n = 5 mice per group).

increased in the body when metabolism of cysteine or methionine is impaired. So our results clearly showed that I/R interfered with the methionine metabolism directly or indirectly and altered the methionine metabolizing enzymes that lead to hyperhomocysteinemia (HHcy). During HHcy, Hcy may be translocated to the mitochondria and induce hypermethylation by increasing SAHH and decreasing MTHFR levels (Fig. 4). However, THC treatment ameliorated these changes. Overall, our data suggest that an increased Hcy level may play a significant role in the altered expression of methionine metabolizing enzymes during ischemia and the protective role of THC in this matter.

It has been reported that HHcy is known to contribute to oxidative damage of cellular organelles such as mitochondria (Tyagi et al., 2005), however the effect of HHcy on mitochondrial dynamics and dysfunction particularly in ischemic mitochondria and its consequence on brain function has not come into question in the literature. It is known that Hcy induces cerebral arteriolar stiffness, endothelium damage and finally brain dysfunction (Nappo et al., 1999). In our study, the levels of mitochondrial $p47^{phox}$, $gp91^{phox}$ (oxidative stress) were increased and levels of Trx-2, MnSOD (anti-oxidant) were decreased, respectively, in the ischemic mitochondrial fraction and treatment with THC mitigated these levels of oxidative stress (Fig. 5). Because THC is an antioxidant (Rajeswari, 2006), treatment of THC in animals with I/R injury will result in amelioration of mitochondrial dysfunction through minimizing oxidative stress.

It is well known that mitochondria have the primary function of providing cellular chemical energy in the form of ATP by oxidative phosphorylation via the electron transport chain, and as such they have been termed the cells' "powerhouse" (Watts et al., 2013). The mitochondrial permeability transition (MPT) results from opening of a pore in the inner mitochondrial membrane that is non-selectively permeable to solutes smaller than 1.5 kDa (Halestrap, 2006; Leung and Halestrap, 2008; Tsujimoto et al., 2006; Sims and Muyderman, 2010). Transition pore opening can be promoted by multiple factors including oxidative stress. Cell damage resulting from conditions such as neurodegenerative diseases and head injury, cause an opening of the mitochondrial permeability transition pore, which can greatly reduce ATP production and can cause ATP synthase to begin hydrolysing, rather than producing, ATP (Stavrovskaya and Kristal, 2005). Moreover, alternation in MPT can alter the rate of oxygen consumption. Cerebral tissue damage due to ischemic reperfusion injury causes disruption to the delivery of glucose and oxygen, leading to greatly reduced ATP generation. In conformity with the above facts, we noticed an increase in brain MTP and subsequent decrease in O_2 consumption leading to reduction in ATP production in ischemic stroke while treatment with THC ameliorated these changes (Fig. 6).

In our study, we noticed a significant increase in matrix metalloproteinase-9 (MMP-9) activity in the mitochondrial fraction isolated from the ischemic brain of I/R mice compared to sham. Interestingly, THC treatment was able to significantly reduce the MMP-9 activity in the I/R + THC group compared to I/R only (Fig. 7). MMP-9, a member of the MMP family that normally remodels the extracellular matrix, has been shown to play an important role in both animal models of cerebral ischemia and human stroke (Dong et al., 2009). The expression of MMP-9 is elevated after cerebral ischemia, which is involved in accelerating matrix degradation, disrupting the BBB integrity and increasing the infarct size during stroke. MMP expression can be regulated by enzyme inhibitors. The endogenous inhibitors of MMP-9 are tissue inhibitors of metalloproteinase (TIMPs: TIMP-1 and TIMP-2) (Romanic et al., 1998). Thus, the balance between MMPs and TIMPs is critical for proper ECM remodeling and is essential for several developmental and morphogenetic processes (Dollery et al., 1999). In our study, we did not notice any significant change ($p > 0.05$) in TIMP-1 protein and mRNA levels between the three experimental mice groups. However, we noticed a significant decrease in TIPM-2 proteins in the I/R group compared to sham and THC treatment ameliorated these changes. Gene expression via RT-qPCR analysis also revealed reduced TIMP-2 expression in the ischemic brain (Fig. 7). The present study, along with earlier reports, suggested a substantial increase in MMP-9 expression and with decreased expression of its inhibitor TIMP-2 (Refsum et al., 1998). Furthermore, the increased MMP-9 protein/mRNA levels caused degradation of tight junction proteins (TJPs) and led to an increase in BBB permeability. TJPs play an important role in tissue integrity but also in vascular permeability, leukocyte extravasation and angiogenesis (Tyagi et al., 2006). The TJPs regulate BBB function and maintain mitochondrial permeability transition (MPT) pores in a closed state, which gives it a neuroprotective property. We noticed the activation of MMP-9 is associated with reduced expression of cellular tight junction proteins and mRNA (ZO1 and Occludin) leading to mitophagy. The results showed down regulation of ZO1 and Occludin via mitochondria dysfunction the ischemic brain, which was mitigated by THC treatment (Fig. 7). These results suggest THC treatment reversed the effect of ischemia on cerebral vascular injury, in part, by inhibiting MMPs/TIMPs, thus preventing TJP degradation preserving vascular integrity.

It is well known that timely removal of damaged mitochondria via autophagy (mitophagy) is critical for cellular homeostasis and function (Ni et al., 2014). Mitochondria are reticular organelles that have high plasticity for their dynamic structures and constantly undergo fission and fusion to repair damaged components of the mitochondria, which allows for segregation of damaged mitochondria via the fission process and exchange of material between healthy mitochondria via the fusion process (Van der Bliek et al., 2013; Twig, 2008). In this study, we have demonstrated that THC ameliorates mitophagy in brain mitochondria of mice after cerebral ischemia/reperfusion injury (Fig. 8). Thus, inhibition of mitophagy through THC treatment may help to reduce ischemic injury.

It has been reported that ischemia leads to huge alterations in gene expression (Schweizer et al., 2013). Augmented transcriptional repression can be noticed together with the corresponding silencing epigenetic marks. According to previous reports, after an ischemic insult, the global amount of DNA methylation raises and this increase correlates with augmented brain injury (Endres et al., 2000). Thus, the manipulation of transcription on the epigenetic level can yield a protective state. A body of evidence is accumulating, proving that epigenetic modifications regulate a wide range of neuro-physiologic as well as neuro-pathologic processes (Schweizer et al., 2013). In the brain, the epigenetic machinery covers basic phenomena such as differentiation, the preservation of tissue specific transcription profiles, as well as complex processes from synaptic plasticity to learning and memory (Levenson et al., 2004). DNA methylation occurs at CpG islands. The methylation step is carried out by DNA methyltransferases (DNMTs) and the subsequent repressive effect is mediated by the recruitment of chromatin modifiers that bind to the methylated site (Doerfler, 2008). In our study, we noticed that DNMT1 and DNMT3a proteins and gene expressions along with overall brain DNMT activity were drastically increased in ischemic mitochondria compared to sham and treatment with THC ameliorated these changes (Fig. 9). To further test the mechanism of THC induced DNMT normalization in ischemic mitochondria, we measured the DNMT levels in ischemic mice treated with DNMT inhibitor (5-Aza) and found recovery of DNMT levels close to that of the sham group (Fig. 9).

We also showed that, the SAM/SAH ratio was significantly higher in the ischemic brain compared to sham (Fig. 4). MMP-9 activity was increased in ischemic mitochondria followed by the subsequent downregulation of TIMP-2 compared to sham (Fig. 7). Downregulation of TIMP-2 expression in ischemic mitochondria tempts us to further investigate the possibility of epigenetic silencing of this gene expression. Bioinformatics analysis identified a CpG island is present in the TIMP gene promoter locus (Fig. 9). The qMSP confirmed the high degree of DNA methylation, called hyper-methylation in the CpG island of TIMP-2 promoter under I/R condition. Our data clearly indicated that TIMP-2 protein expression was significantly reduced, through increased DNA hyper-methylation and epigenetic suppression of gene transcription. To study further evidence of DNA methylation, we noticed higher global DNA methylation (% of 5-mC level) of the genome using 5-mC ELISA (Fig. 9). Furthermore, to acquire evidence explaining the role of DNA methylation during ischemia in the expression of TIMP-2, we treated DNA methylation inhibitor 5-azacytidine (5-Aza) to I/R mice, which specifically inhibits DNMTs. We noticed that the5-Aza and THC treatment significantly altered TIMP-2 production in the ischemic condition as compared to sham (Fig. 9). Together, the results demonstrate that epigenetic DNA hyper-methylation was triggered during ischemic reperfusion injury, leading to TIMP-2 suppression and ECM remodeling.

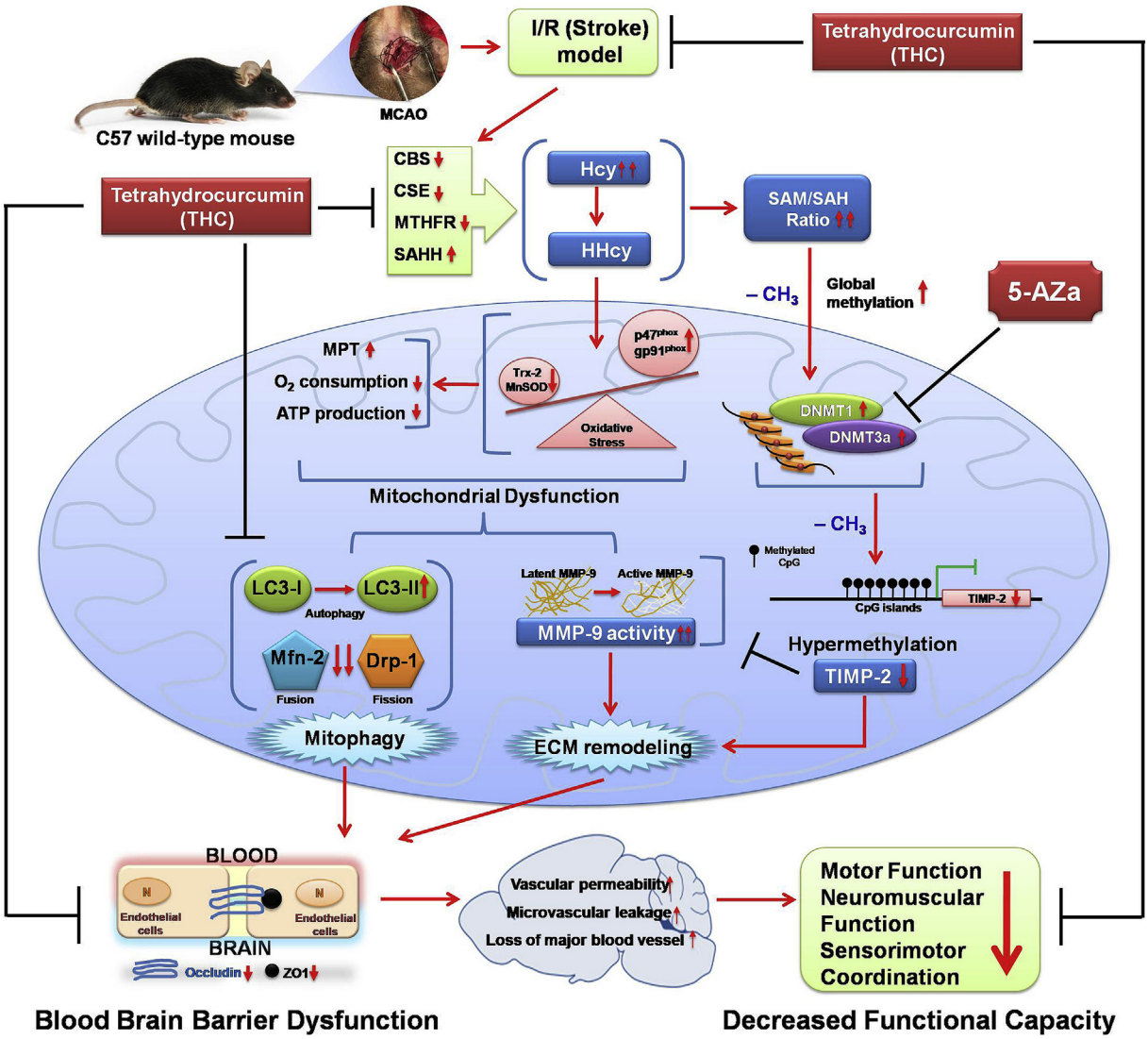

Fig. 10. Diagrammatic representation of the overall study finding.

The overall summary of all of the research findings is presented in Fig. 10. Our study clearly indicates that ischemic reperfusion injury in the wild type mouse can exert its deleterious effect on the brain by executing hyperhomocysteinemia (HHcy) phenotypes. HHcy augments mitochondrial oxidative stress as evident from elevated expression of oxidants and depleted antioxidants in mitochondrial fractions isolated from the ischemic brain. Thus, the observed imbalance between oxidants and antioxidants poses a greater threat of oxidative injury and subsequent mitochondrial dysfunction. Additionally, mitochondrial oxidative stress was found to be linked with increased mitochondrial permeability transition, reduced oxygen consumption and subsequent decrease in ATP production leading to mitochondrial dysfunction. Elevated mitochondrial oxidative stress was found to be positively linked with autophagy, fusion, fission and elevated MMP-9 activity in ischemic mitochondria leading to mitophagy and ECM damage. On the other hand, in ischemic mice, elevated Hcy levels in the brain was linked with an increased SAM/SAH ratio, which in turn increased the global DNA methylation leading to elevated expression of DNMT1 and DNMT3a. DNMTs transfers more methyl ($-CH_3$) groups in the CpG islands of the TIMP-2 promoter leading to reduced TIMP-2 expression in ischemic mitochondria. TIMP-2 was found to inhibit MMP-9 activity but because of its reduced expression in ischemic brain mitochondria, MMP-9 activity remained elevated. Mechanistic studies showed that treatment of DNMT inhibitor (5-Aza) in ischemic mice can abolish the pathway of TIMP-2 hyper-methylation. Collectively, the observed mitophagy and ECM remodeling can be responsible for blood brain barrier damage, which in turn increased vascular permeability, microvascular leakage and loss of major blood vessels in the ischemic brain. Thus motor function, neuromuscular function and sensorimotor coordination were hampered in ischemic mice. THC, being a potent antioxidant, was found to inhibit these mechanisms of mitochondrial dysfunction, TIMP-2 hypermethylation and subsequent recovery of functional capacity in mice with ischemic reperfusion injury. Therefore, THC treatment is found to be a powerful preventive and therapeutic approach for ischemia that has both tremendous molecular and physiological functions.

Conflicts of interest

The authors declare that they have no conflicts of interest.

Acknowledgements

The study was supported in part by National Institutes of Health (NIH) grants HL-107640 and AR-067667.

Appendix A. Supplementary data

Supplementary data to this article can be found online at https://doi.org/10.1016/j.neuint.2018.11.015.

References

Abe, K., Yuki, S., Kogure, K., 1988. Strong attenuation of ischemic and post ischemic brain edema in rats by a novel free radical scavenger. Stroke 19, 480–485.

AHA/ASA stroke statistics, 2016. http://www.strokeassociation.org/STROKEORG/AboutStroke/Impact-of-Stroke-Stroke-statistics_UCM_310728_Article.jsp#.

Arnao, V., Acciarresi, M., Cittadini, E., Caso, V., 2016. Stroke incidence, prevalence and mortality in women worldwide. Int. J. Stroke 11, 287–301.

Beal, M.F., Brouillet, E., Jenkins, B.G., Ferrante, R.J., Kowall, N.W., Miller, J.M., Storey, E., Srivastava, R., Rosen, B.R., Hyman, B.T., 1993. Neurochemical and histologic characterization of striatal excitotoxic lesions produced by the mitochondrial toxin 3-nitropropionic acid. J. Neurosci. 13, 4181–4192.

Bederson, J.B., Pitts, L.H., Tsuji, M., Nishimura, M.C., Davis, R.L., Bartkowski, H., 1986. Rat middle cerebral-artery occlusion: evaluation of the model and development of a neurologic examination. Stroke 17, 472–476.

Behera, J., George, A.K., Voor, M.J., Tyagi, S.C., Tyagi, N., 2018. Hydrogen sulfide epigenetically mitigates bone loss through OPG/RANKL regulation during hyperhomocysteinemia in mice. Bone 114, 90–108.

Belayev, L., Busto, R., Zhao, W., Ginsberg, M.D., 1996. Quantitative evaluation of blood-brain barrier permeability following middle cerebral artery occlusion in rats. Brain Res. 739, 88–96.

Bostom, A.G., Rosenberg, I.H., Silbershatz, H., Jacques, P.F., Selhub, J., D'Agostino, R.B., Wilson, P.W., Wolf, P.A., 1999. Nonfasting plasma total homocysteine levels and stroke incidence in elderly persons: the Framingham Study. Ann. Intern. Med. 131, 352–355.

Casas, J.P., Bautista, L.E., Smeeth, L., Sharma, P., Hingorani, A.D., 2005. Homocysteine and stroke: evidence on a causal link from Mendelian randomisation. Lancet 365, 224–232.

Chen, H., Chan, D.C., 2009. Mitochondrial dynamics–fusion, fission, movement, and mitophagy–in neurodegenerative diseases. Hum. Mol. Genet. 18, R169–R176.

Chen, H., Yoshioka, H., Kim, G.S., Jung, J.E., Okami, N., Sakata, H., Maier, C.M., Narasimhan, P., Goeders, C.E., Chan, P.H., 2011. Oxidative stress in ischemic brain damage: mechanisms of cell death and potential molecular targets for neuroprotection. Antioxidants Redox Signal. 14, 1505–1517.

Crabbe, J.C., Metten, P., Yu, C.H., Schlumbohm, J.P., Cameron, A.J., Wahlsten, D., 1985. Genotypic differences in ethanol sensitivity in two tests of motor in coordination. J. Appl. Physiol. 95, 1338–1351.

Cui, R., Moriyama, Y., Koike, K.A., Date, C., Kikuchi, S., Tamakoshi, A., Iso, H., JACC Study group, 2007. Serum total homocysteine concentrations and risk of mortality from stroke and coronary heart disease in Japanese: the JACC study. Atherosclerosis 198, 412–418.

Dawson, T.L., Gores, G.J., Nieminen, A.L., Herman, B., Lemasters, J.J., 1993. Mitochondria as a source of reactive oxygen species during reductive stress in rat hepatocytes. Am. J. Physiol. 264, C961–C967.

De Luca, A.M., 2008. Use of grip strength meter to assess the limb strength of mdx mice. SOP DMD_M.2.2.001. http://www.treat-nmd.eu/downloads/file/sops/dmd/MDX/DMD_M.2.2.001.pdf.

Dirnagl, Ulrich, Group, Members of the MCAO-SOP, 2009. Standard operating procedures (SOP) in experimental stroke research: SOP for middle cerebral artery occlusion in the mouse. http://hdl.handle.net/10101/npre.2009.3492.1.

Doerfler, W., 2008. In pursuit of the first recognized epigenetic signal–DNA methylation: a 1976 to 2008 synopsis. Epigenetics 3, 125–133.

Dollery, C.M., Humphries, S.E., McClelland, A., Latchman, D.S., McEwan, J.R., 1999. Expression of tissue inhibitor of matrix metalloproteinases 1 by use of an adenoviral vector inhibits smooth muscle cell migration and reduces neointimal hyperplasia in the rat model of vascular balloon injury. Circulation 99, 3199–3205.

Dong, X., Song, Y.N., Liu, W.G., Guo, X.L., 2009. Mmp-9, a potential target for cerebral ischemic treatment. Curr. Neuropharmacol. 7, 269–275.

Endres, M., Meisel, A., Biniszkiewicz, D., Namura, S., Prass, K., Ruscher, K., Lipski, A., Jaenisch, R., Moskowitz, M.A., Dirnagl, U., 2000. DNA methyltransferase contributes to delayed ischemic brain injury. J. Neurosci. 20, 3175–3181.

Fukui, S., Fazzina, G., Amorini, A.M., Dunbar, J.G., Marmarou, A., 2003. Differential effects of atrial natriuretic peptide on the brain water and sodium after experimental cortical contusion in the rat. J. Cerebr. Blood Flow Metabol. 23, 1212–1218.

Gasche, Y., Copin, J.C., Sugawara, T., Fujimura, M., Chan, P.H., 2001. Matrix metalloproteinase inhibition prevents oxidative stress-associated blood-brain barrier disruption after transient focal cerebral ischemia. J. Cerebr. Blood Flow Metabol. 21, 1393–1400.

Gasche, Y., Fujimura, M., Morita-Fujimura, Y., Copin, J.C., Kawase, M., Massengale, J., Chan, P.H., 1999. Early appearance of activated matrix metalloproteinase-9 after focal cerebral ischemia in mice: a possible role in blood-brain barrier dysfunction. J. Cerebr. Blood Flow Metabol. 19, 1020–1028.

George, A.K., Behera, J., Kelly, K.E., Mondal, N.K., Richardson, K.P., Tyagi, N., 2018. Exercise mitigates alcohol induced endoplasmic reticulum stress mediated cognitive impairment through ATF6-herp signaling. Sci. Rep. 8, 5158.

Givvimani, S., Sen, U., Tyagi, N., Munjal, C., Tyagi, S.C., 2011. X-ray imaging of differential vascular density in MMP-9-/-, PAR-1-/+, hyperhomocysteinemic (CBS-/+) and diabetic (Ins 2-/+) mice. Arch. Physiol. Biochem. 117, 1–7.

Gores, G.J., Flarsheim, C.E., Dawson, T.L., Nieminen, A.L., Herman, B., Lemasters, J.J., 1989. Swelling, reductive stress, and cell death during chemical hypoxia in hepatocytes. Am. J. Physiol. 257, C347–C354.

Graber, T.G., Ferguson-Stegall, L., Kim, J.-H., Thompson, L.V., 2013. C57BL/6 neuromuscular health span scoring system. J. Gerontol. Biol. Med. Sci. 68, 1326–1336.

Graber, T.G., Rawls, B.L., Tian, B., Durham, W.J., Brightwell, C.R., Brasier, A.R., Rasmussen, B.B., Fry, C.S., 2018. Repetitive TLR3 activation in the lung induces skeletal muscle adaptations and cachexia. Exp. Gerontol. 106, 88–100.

Hagberg, H., Mallard, C., Rousset, C.I., Thornton, C., 2014. Mitochondria: hub of injury responses in the developing brain. Lancet Neurol. 13, 217–232.

Halestrap, A.P., 2006. Calcium, mitochondria and reperfusion injury: a pore way to die. Biochem. Soc. Trans. 34, 232–237.

Haley, M.J., Lawrence, C.B., 2017. The blood-brain barrier after stroke: structural studies and the role of transcytotic vesicles. J. Cerebr. Blood Flow Metabol. 37, 456–470.

Hamacher-Brady, A., Brady, N.R., Gottlieb, R.A., 2006. Enhancing macroautophagy protects against ischemia/reperfusion injury in cardiac myocytes. J. Biol. Chem. 281, 29776–29787.

Iso, H., Moriyama, Y., Sato, S., Kitamura, A., Tanigawa, T., Yamagishi, K., Imano, H., Ohira, T., Okamura, T., Naito, Y., Shimamoto, T., 2004. Serum total homocysteine concentrations and risk of stroke and its subtypes in Japanese. Circulation 109, 2766–2772.

Kalani, A., Kamat, P.K., Givvimani, S., Brown, K., Metreveli, N., Tyagi, S.C., Tyagi, N., 2014. Nutri-epigenetics ameliorates blood-brain barrier damage and neurodegeneration in hyperhomocysteinemia: role of folic acid. J. Mol. Neurosci. 52, 202–215.

Kamat, P.K., Kalani, A., Givvimani, S., Sathnur, P.B., Tyagi, S.C., Tyagi, N., 2013. Hydrogen sulfide attenuates neurodegeneration and neurovascular dysfunction induced by intracerebral-administered homocysteine in mice. Neuroscience 252, 302–319.

Kamat, P.K., Kalani, A., Metreveli, N., Tyagi, S.C., Tyagi, N., 2015. A possible molecular mechanism of hearing loss during cerebral ischemia in mice. Can. J. Physiol. Pharmacol. 93, 505–516.

Kleinschnitz, C., Schwab, N., Kraft, P., Hagedorn, I., Dreykluft, A., Schwarz, T., Austinat, M., Nieswandt, B., Wiendl, H., Stoll, G., 2010. Early detrimental T-cell effects in experimental cerebral ischemia are neither related to adaptive immunity nor thrombus formation. Blood 115, 3835–3842.

Larcher, T., Lafoux, A., Tesson, L., Remy, S., Thepenier, V., François, V., Le Guiner, C., Goubin, H., Dutilleul, M., Guigand, L., Toumaniantz, G., De Cian, A., Boix, C., Renaud, J.B., Cherel, Y., Giovannangeli, C., Concordet, J.P., Anegon, I., Huchet, C., 2014. Characterization of dystrophin deficient rats: a new model for Duchenne muscular dystrophy. PLoS One 9, e110371.

Leung, A.W., Halestrap, A.P., 2008. Recent progress in elucidating the molecular mechanism of the mitochondrial permeability transition pore. Biochim. Biophys. Acta 1777, 946–952.

Levenson, J.M., O'Riordan, K.J., Brown, K.D., Trinh, M.A., Molfese, D.L., Sweatt, J.D., 2004. Regulation of histone acetylation during memory formation in the hippocampus. J. Biol. Chem. 279, 40545–40559.

Li, Q., Gao, S., 2017. Mitochondrial dysfunction in ischemic stroke. In: Lapchak, P., Yang, G.Y. (Eds.), Translational Research in Stroke. Translational Medicine Research. Springer, Singapore. https://doi.org/10.1007/978-981-10-5804-2_10.

Liu, Z., Xie, Z., Jones, W., Pavlovicz, R.E., Liu, S., Yu, J., Li, P.K., Lin, J., Fuchs, J.R., Marcucci, G., Li, C., Chan, K.K., 2009a. Curcumin is a potent DNA hypomethylation agent. Bioorg. Med. Chem. Lett 19, 706–709.

Liu, F., Yuan, R., Benashski, S.E., McCullough, L.D., 2009b. Changes in experimental stroke outcome across the life span. J. Cerebr. Blood Flow Metabol. 29, 792–802.

Lominadze, D., Roberts, A.M., Tyagi, N., Moshal, K.S., Tyagi, S.C., 2006. Homocysteine causes cerebrovascular leakage in mice. Am. J. Physiol. Heart Circ. Physiol. 290, H1206–H1213.

Longa, E.Z., Weinstein, P.R., Carlson, S., Cummins, R., 1989. Reversible middle cerebral artery occlusion without craniectomy in rats. Stroke 20, 84–91.

Lu, P., Takai, K., Weaver, V.M., Werb, Z., 2011. Extracellular matrix degradation and remodeling in development and disease. Cold Spring Harb. Perspect. Biol. 3https://doi.org/10.1101/cshperspect.a005058. pii: a005058.

Mehler, M.F., 2008. Epigenetic principles and mechanisms underlying nervous system functions in health and disease. Prog. Neurobiol. 86, 305–341.

Mishra, S., Mishra, M., Seth, P., Sharma, S.K., 2010. Tetrahydrocurcumin confers protection against amyloid beta-induced toxicity. Neuroreport 22, 23–27.

Mishra, S., Palanivelu, K., 2008. The effect of curcumin (turmeric) on Alzheimer's disease: an overview. Ann. Indian Acad. Neurol. 11, 13–19.

Moshal, K.S., Tipparaju, S.M., Vacek, T.P., Kumar, M., Singh, M., Frank, I.E., Patibandla, P.K., Tyagi, N., Rai, J., Metreveli, N., Rodriguez, W.E., Tseng, M.T., Tyagi, S.C., 2008. Mitochondrial matrix metalloproteinase activation decreases myocyte contractility in hyperhomocysteinemia. Am. J. Physiol. Heart Circ. Physiol. 295, H890–H897.

Muradashvili, N., Benton, R.L., Saatman, K.E., Tyagi, S.C., Lominadze, D., 2015. Ablation of matrix metalloproteinase-9 gene decreases cerebrovascular permeability and fibrinogen deposition post traumatic brain injury in mice. Metab. Brain Dis. 30, 411–426.

Murugan, P., Pari, L., Rao, C.A., 2008. Effect of tetrahydrocurcumin on insulin receptor status in type2diabeticrats: studies on insulin binding to erythrocytes. J. Biosci. 33, 63–72.

Myojin, K., Taguchi, A., Umetani, K., Fukushima, K., Nishiura, N., Matsuyama, T., Kimura, H., Stern, D.M., Imai, Y., Mori, H., 2007. Visualization of intracerebral arteries by synchrotron radiation micro angiography. AJNR. Am. J. Neuroradiol. 28, 953–957.

Namekata, K., Enokido, Y., Ishii, I., Nagai, Y., Harada, T., Kimura, H., 2004. Abnormal lipid metabolism in cystathionine beta-synthase-deficient mice, an animal model for hyperhomocysteinemia. J. Biol. Chem. 279, 52961–52969.

Nappo, F., De, R.N., Marfella, R., De, L.D., Ingrosso, D., Perna, A.F., Farzati, B., Giugliano,

D., 1999. Impairment of endothelial functions by acute hyperhomocysteinemia and reversal by antioxidant vitamins. J. Am. Med. Assoc. 281, 2113–2118.
Ni, H.M., Williams, J.A., Ding, W.X., 2014. Mitochondrial dynamics and mitochondrial quality control. Redox. Biol. 4, 6–13.
Pastorino, J.G., Snyder, J.W., Serroni, A., Hoek, J.B., Farber, J.L., 1993. Cyclosporin and carnitine prevent the anoxic death of cultured hepatocytes by inhibiting the mitochondrial permeability transition. J. Biol. Chem. 268, 13791–13798.
Pushpakumar, S., Kundu, S., Pryor, T., Givvimani, S., Lederer, E., Tyagi, S.C., Sen, U., 2013. Angiotensin-II induced hypertension and renovascular remodelling in tissue inhibitor of metalloproteinase 2 knockout mice. J. Hypertens. 31, 2270–2281.
Qipshidze, N., Tyagi, N., Sen, U., Givvimani, S., Metreveli, N., Lominadze, D., Tyagi, S.C., 2010. Folic acid mitigated cardiac dysfunction by normalizing the levels of tissue inhibitor of metalloproteinase and homocysteine-metabolizing enzymes post myocardial infarction in mice. Am. J. Physiol. Heart Circ. Physiol. 299, H1484–H1493.
Qureshi, I.A., Mehler, M.F., 2010. Emerging role of epigenetics in stroke: part 1: DNA methylation and chromatin modifications. Arch. Neurol. 67, 1316–1322.
Rajeswari, A., 2006. Curcumin protects mouse brain from oxidative stress caused by 1-methyl-4-phenyl-1,2,3,6-tetrahydropyridine. Eur. Rev. Med. Pharmacol. Sci. 10, 157–161.
Refsum, H., Ueland, P.M., Nygard, O., Vollset, S.E., 1998. Homocysteine and cardiovascular disease. Annu. Rev. Med. 49, 31–62.
Rodrigues, T., Santos, A.C., Pigoso, A.A., Mingatto, F.E., Uyemura, S.A., Curti, C., 2002. Thioridazine interacts with the membrane of mitochondria acquiring antioxidant activity toward apoptosis–potentially implicated mechanisms. Br. J. Pharmacol. 136, 136–142.
Romanic, A.M., White, R.F., Arleth, A.J., Ohlstein, E.H., Barone, F.C., 1998. Matrix metalloproteinase expression increases after cerebral focal ischemia in rats: inhibition of matrix metalloproteinase-9 reduces infarct size. Stroke 29, 1020–1030.
Römer, C., Engel, O., Winek, K., Hochmeister, S., Zhang, T., Royl, G., Klehmet, J., Dirnagl, U., Meisel, C., Meisel, A., 2015. Blocking stroke-induced immunodeficiency increases CNS antigen-specific auto reactivity but does not worsen functional outcome after experimental stroke. J. Neurosci. 35, 7777–7794.
Sacco, R.L., Anand, K., Lee, H.S., Boden-Albala, B., Stabler, S., Allen, R., Paik, M.C., 2004. Homocysteine and the risk of ischemic stroke in a triethnic cohort: the Northern Manhattan Study. Stroke 35, 2263–2269.
Schaar, K.L., Brenneman, M.M., Savitz, S.I., 2010. Functional assessments in the rodent stroke model. Exp. Transl. Stroke Med. 2, 13. https://doi.org/10.1186/2040-7378-2-13.
Schallert, T., Fleming, S.M., Leasure, J.L., Tillerson, J.L., Bland, S.T., 2000. CNS plasticity and assessment of forelimb sensorimotor outcome in unilateral rat models of stroke, cortical ablation, Parkinsonism and spinal cord injury. Neuropharmacology 39, 777–787.
Schweizer, S., Meisel, A., Märschenz, S., 2013. Epigenetic mechanisms in cerebral ischemia. J. Cerebr. Blood Flow Metabol. 33, 1335–1346.
Sen, U., Basu, P., Abe, O.A., Givvimani, S., Tyagi, N., Metreveli, N., Shah, K.S., Passmore, J.C., Tyagi, S.C., 2009. Hydrogen sulfide ameliorates hyperhomocysteinemia-associated chronic renal failure. Am. J. Physiol. Renal. Physiol. 297, F410–F419.
Shi, Z., Guan, Y., Huo, Y.R., Liu, S., Zhang, M., Lu, H., Yue, W., Wang, J., Ji, Y., 2015. Elevated total homocysteine levels in acute ischemic stroke are associated with long-term mortality. Stroke 46, 2419–2425.
Sims, N.R., Muyderman, H., 2010. Mitochondria, oxidative metabolism and cell death in stroke. Biochim. Biophys. Acta 1802, 80–91.
Stavrovskaya, I.G., Kristal, B.S., 2005. The powerhouse takes control of the cell: is the mitochondrial permeability transition a viable therapeutic target against neuronal dysfunction and death? Free Radic. Biol. Med. 38, 687–697.
Tsujimoto, Y., Nakagawa, T., Shimizu, S., 2006. Mitochondrial membrane permeability transition and cell death. Biochim. Biophys. Acta Bioenerg. 1757, 1297–1300.
Twig, G., 2008. Fission and selective fusion govern mitochondrial segregation and elimination by autophagy. EMBO J. 27, 433–446.
Tyagi, N., Moshal, K.S., Sen, U., Vacek, T.P., Kumar, M., Hughes Jr., W.M., Kundu, S., Tyagi, S.C., 2009. H_2S protects against methionine-induced oxidative stress in brain endothelial cells. Antioxidants Redox Signal. 11, 25–33.
Tyagi, N., Ovechkin, A.V., Lominadze, D., Moshal, K.S., Tyagi, S.C., 2006. Mitochondrial mechanism of microvascular endothelial cells apoptosis in hyperhomocysteinemia. J. Cell. Biochem. 98, 1150–1162.
Tyagi, N., Qipshidze, N., Munjal, C., Vacek, J.C., Metreveli, N., Givvimani, S., Tyagi, S.C., 2012. Tetrahydrocurcumin ameliorates homocysteinylated cytochrome-c mediated autophagy in hyperhomocysteinemia mice after cerebral ischemia. J. Mol. Neurosci. 47, 128–138.
Tyagi, N., Sedoris, K.C., Steed, M., Ovechkin, A.V., Moshal, K.S., Tyagi, S.C., 2005. Mechanisms of homocysteine-induced oxidative stress. Am. J. Physiol. Heart Circ. Physiol. 289, H2649–H2656.
Tyagi, N., Vacek, J.C., Givvimani, S., Sen, U., Tyagi, S.C., 2010. Cardiac specific deletion of N-methyl-d-aspartate receptor 1 ameliorates mtMMP-9 mediated autophagy/mitophagy in hyperhomocysteinemia. J. Recept. Signal Transduct. Res. 30, 78–87.
Utepbergenov, D.I., Mertsch, K., Sporbert, A., Tenz, K., Paul, M., Haseloff, R.F., Blasig, I.E., 1998. Nitric oxide protects blood-brain barrier in vitro from hypoxia/reoxygenation-mediated injury. FEBS Lett. 424, 197–201.
Utsumi, K., Amemiya, S., Iizuka, M., Iino, Y., Katayama, Y., 2003. Acute posterior leukoencephalopathy in a patient with nephrotic syndrome. Clin. Exp. Nephrol. 7, 63–66.
Uyama, O., Okamura, N., Yanase, M., Narita, M., Kawabata, K., Sugita, M., 1988. Quantitative evaluation of vascular permeability in the gerbil brain after transient ischemia using Evans blue fluorescence. J. Cerebr. Blood Flow Metabol. 8, 282–284.
Van der Bliek, A.M., Shen, Q., Kawajiri, S., 2013. Mechanisms of mitochondrial fission and fusion. Cold Spring Harbor Perspectives in Biology 5.
van der Wijst, M.G., Rots, M.G., 2015. Mitochondrial epigenetics: an overlooked layer of regulation? Trends Genet. 31, 353–356.
Veltkamp, R., Siebing, D.A., Sun, L., Heiland, S., Bieber, K., Marti, H.H., Nagel, S., Schwab, S., Schwaninger, M., 2005. Hyperbaric oxygen reduces blood-brain barrier damage and edema after transient focal cerebral ischemia. Stroke 36, 1679–1683.
Wald, D.S., Law, M., Morris, J.K., 2002. Homocysteine and cardiovascular disease: evidence on causality from a meta-analysis. Br. Med. J. 325, 1202–1206.
Wang, L., Jhee, K.H., Hua, X., DiBello, P.M., Jacobsen, D.W., Kruger, W.D., 2004. Modulation of cystathionine beta-synthase level regulates total serum homocysteine in mice. Circ. Res. 94, 1318–1324.
Wang, W., Upshaw, L., Strong, D.M., Robertson, R.P., Reems, J., 2005. Increased oxygen consumption rates in response to high glucose detected by a novel oxygen biosensor system in non-human primate and human islets. J. Endocrinol. 185, 445–455.
Watts, L.T., Lloyd, R., Garling, R.J., Duong, T., 2013. Stroke neuroprotection: targeting mitochondria. Brain Sci. 3, 540–560.
Wilson-Fritch, L., Nicoloro, S., Chouinard, M., Lazar, M.A., Chui, P.C., Leszyk, J., Straubhaar, J., Czech, M.P., Corvera, S., 2004. Mitochondrial remodeling in adipose tissue associated with obesity and treatment with rosiglitazone. J. Clin. Invest. 114, 1281–1289.
Yodkeeree, S., Garbisa, S., Limtrakul, P., 2008. Tetrahydrocurcumin inhibits HT1080 cell migration and invasion via downregulation of MMPs and uPA. Acta Pharmacol. Sin. 29, 853–860.
Zahrebelski, G., Nieminen, A.L., al-Ghoul, K., Qian, T., Herman, B., Lemasters, J.J., 1995. Progression of sub cellular changes during chemical hypoxia to cultured rat hepatocytes: a laser scanning confocal microscopic study. Hepatology 21, 1361–1372.